Am J Nucl Med Mol Imaging 2016;6(5):234-261
www.ajnmmi.us /ISSN:2160-8407/ajnmmi0034773

Review Article

Genetic engineered molecular imaging probes for applications in cell therapy: emphasis on MRI approach

In K Cho[1,2], Silun Wang[3], Hui Mao[3], Anthony WS Chan[1,2]

[1]Department of Human Genetics, Emory University School of Medicine, Atlanta, GA, USA; [2]Division of Neuropharmacology and Neurologic Diseases, Yerkes National Primate Research Center, Atlanta, GA, USA; [3]Department of Radiology and Imaging Sciences, Emory University School of Medicine, Atlanta, GA, USA

Received August 12, 2016; Accepted August 31, 2016; Epub September 22, 2016; Published September 30, 2016

Abstract: Recent advances in stem cell-based regenerative medicine, cell replacement therapy, and genome editing technologies (i.e. CRISPR-Cas 9) have sparked great interest in *in vivo* cell monitoring. Molecular imaging promises a unique approach to noninvasively monitor cellular and molecular phenomena, including cell survival, migration, proliferation, and even differentiation at the whole organismal level. Several imaging modalities and strategies have been explored for monitoring cell grafts *in vivo*. We begin this review with an introduction describing the progress in stem cell technology, with a perspective toward cell replacement therapy. The importance of molecular imaging in reporting and assessing the status of cell grafts and their relation to the local microenvironment is highlighted since the current knowledge gap is one of the major obstacles in clinical translation of stem cell therapy. Based on currently available imaging techniques, we provide a brief discussion on the pros and cons of each imaging modality used for monitoring cell grafts with particular emphasis on magnetic resonance imaging (MRI) and the reporter gene approach. Finally, we conclude with a comprehensive discussion of future directions of applying molecular imaging in regenerative medicine to emphasize further the importance of correlating cell graft conditions and clinical outcomes to advance regenerative medicine.

Keywords: *In vivo* cell monitoring, molecular imaging, reporter gene, magnetic resonance imaging, longitudinal monitoring, stem cell, regenerative medicine, cell tracking

Introduction

With the successful isolation of pluripotent stem cells and their maintenance *in vitro*, stem cell research has advanced dramatically over the past three decades. Various stem cell technologies, including isolation of human embryonic stem cells [1], directed stem cell differentiation [2-4], transdifferentiation [5, 6], induced pluripotent stem cells (iPSC) [7], and successful derivation of patient-specific pluripotent stem cells by somatic cell nuclear transfer [8], underscore the tremendous pace at which stem cell technology is advancing. Stem cells have the potential to be used in fields ranging from, but not limited to, developmental biology, cancer biology, and genetics research to drug discovery and cell replacement therapy.

In the area of regenerative medicine, stem cell-based cell replacement therapy holds a high potential for curing diseases, such as diabetes, bone degenerative diseases, autoimmune diseases, myocardial infarction, brain and spinal cord injuries, and neurodegenerative diseases [9-16]. The primary goal of cell replacement therapy is to replenish damaged or degenerated cell populations. To develop and evaluate the efficacy of cell replacement therapies, it is essential to accurately assess cell survival, proliferation, migration, lineage differentiation, and functional integration at the graft site longitudinally [17-19]. Besides immune rejection and the functionality of cell grafts, one of the major obstacles to clinical translation is current lack of understanding of the fate of implanted cells and how this correlates with clinical outcomes. There is thus an urgent need for tools that allow for noninvasive and longitudinal evaluation of cell grafts. Interest in *in vivo* imaging of cell grafts has soared in the past decade (**Figure**

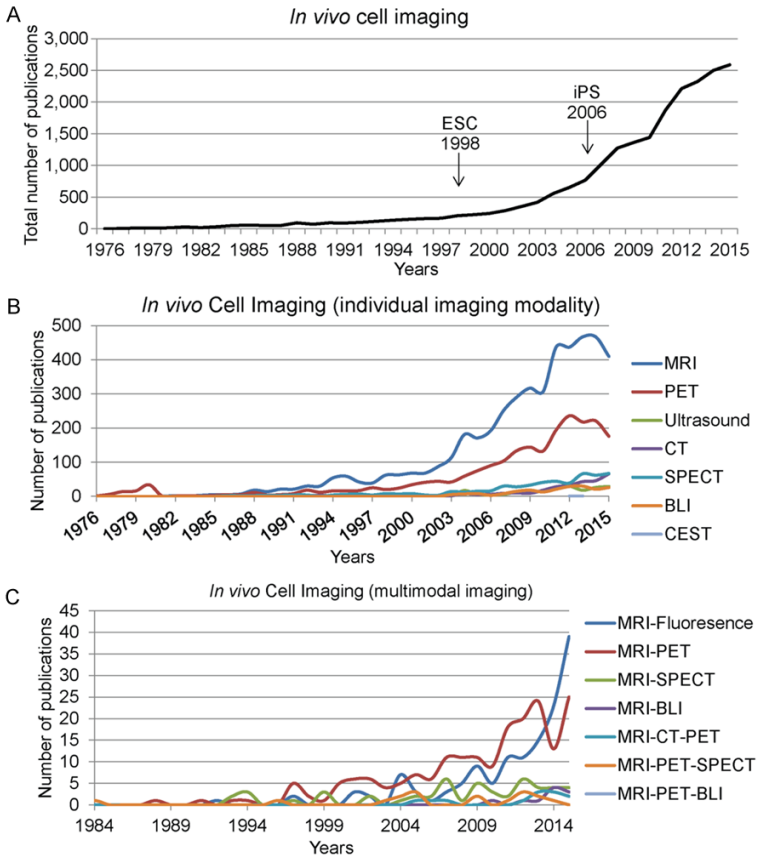

Figure 1. The number of publications by year. A. The total number of publications by year. The PubMed search was conducted using the terms *in vivo* cell, imaging, tracking, or monitoring while excluding terms like reviews, methods, and drug delivery. The years when embryonic stem cells (1998) and induced pluripotent stem cells (2006) were developed are indicated by arrows. B. The number of publications broken down into each imaging modality. C. The number of publications using multimodal imaging methods. Abbreviations: PET-positron emission tomography, MRI-magnetic resonance imaging, BLI-bioluminescence imaging, CT-computed tomography, SPECT-single photon emission CT, CEST-chemical exchange saturation transfer.

1A) on the heels of rapid advances in stem cell technology.

The *in vivo* monitoring of grafted cells was reported first in 1976 [20]. In this inaugural study, leukocytes were extracted from patients, labeled with radioactive indium-111, reintroduced to patients, and followed for two days with a gamma camera [20]. With the development of *lacZ* (β-galactosidase) in 1980 [21] and green fluorescent protein (GFP) in 1994 [22], optical colorimetric and fluorescent reporter genes have since been used extensively in imaging of cellular events although the *in vivo* applications are limited. Today, there are a number of imaging modalities available for *in vivo* cell graft tracking leading to great interests and effort in developing cell tracking probes/reporters for respective imaging modalities, including positron emission tomography (PET) [23, 24], computed tomography (CT) [24], single photon emission CT (SPECT) [25], ultrasound (US) [26, 27], bioluminescence imaging (BLI) [28, 29], fluorescence imaging (FLI) [30-32], magnetic resonance imaging (MRI) [17, 23, 33-39]. Among these available imaging modalities, MRI and PET are the most widely investigated and developed due to their relative greater potentials for human and clinical applications (**Figure 1B**). Recently, various combinations of imaging methods have been investigated for *in vivo* cell imaging (**Figure 1C**).

The focus of this review is on *in vivo* imaging and molecular imaging probes for applications in cell therapy. Therefore, in this review, we provide a brief discussion on the advantages and disadvantages of each imaging modality while giving a specific emphasis on MRI and the reporter gene approach. At the end of this review, we discuss future directions for applying molecular imaging in regenerative medicine and emphasize the importance of correlating cell graft conditions and clinical outcomes to advance regenerative medicine.

Literature search

In preparation for this review, we utilized search databases consisted of PubMed and Google Scholar. Search terms included but not limited to *in vivo* cell imaging, *in vivo* cell tracking, *in vivo* cell monitoring, molecular imaging, reporter gene, longitudinal monitoring, MRI reporter, PET reporter, and CT reporter while excluding drug delivery, patent, and agriculture. All the

Table 1. Attributes of an ideal imaging probe/reporter for *in vivo* stem cell graft monitoring

1.	Nontoxic
2.	Maintenance of pluripotency
3.	High sensitivity
4.	Signal persistence
5.	Specificity
6.	Noninvasive

languages were included. The articles were systematically reviewed for relevance based on the title and abstract.

Basic requirements for an imaging probe/reporter for cell tracking

The characteristics and requirements of an ideal imaging probe/reporter were proposed by Frangioni and Hajjar more than a decade ago [40]. However, given the advancement in imaging technologies, emerging new applications and new imaging methods, natural progression, and paradigm shifts in the field, these information needs to be updated. We consider that the optimized imaging probe/reporters for cell tracking should have specific characteristics as summarized in **Table 1**. An ideal imaging probe/reporter should be biodegradable and safe for biological systems. Also, imaging probes/reporters should not impede the viability of the host cells. Although most imaging contrast materials used for cell labeling, such as nanoparticles, have shown promising results in tracking cell grafts, their long-term safety and biocompatibility are still under investigation. Furthermore, an imaging probe/reporter should have no or minimal impact on cell functions. In the cases of pluripotent stem cells or lineage-specific stem cells (i.e. neural stem cells), a probe/reporter should not affect the differentiation potential of the stem cell [41]. Currently, there is a need to establish a set of standardized functional assessment to evaluate the cell functions after the cell labeling with reporters. Some reports showed no effect on differentiation potential [41-44] while others reported a skewed preference for certain lineage-specific cell types [45-48] in the similar assessment. To enable tracking and monitoring cell grafts at the single-cell level and quantifying cell numbers, an ideal imaging probe/reporter and the accompanying imaging methods should also provide great sensitivity for the detection. High sensitivity is particularly important for monitoring migration of stem cells from the graft site in stem cell therapy. How far the grafted cells can migrate and whether they can localize to the targeted anatomic sites will be the critical evaluation points to assess the successful integration and functionality of the stem cells. To these days, the single cell detection is still limited in a few proof of principle studies, notably using micron-sized iron oxide particles (MPIOs) and superparamagnetic iron oxide (SPIO) particles to label cells for MRI tracking [49, 50]. Since most cell-based therapies need longitudinal monitoring of transplanted cells, the signal persistence during the cell division and migration is another desirable property of an imaging probe/reporter. In the case of SPIO labeled cells, precise quantification remains a challenge because of the continued dilution of SPIO as cells divide, proliferate, and migrate. As required in any molecular and cellular imaging probes, cell tracking also needs to have high specificity with signals rising only from the grafted cells and not from other cells. When cells undergo division, apoptosis, or death, imaging probes used for labeling the cells can be released or lost from the cells and then picked up by adjacent cells or persist in the extracellular matrix and give false-positive signals. A genetically engineered imaging reporter can be expressed in the stem cell, and then stem cell grafts can be tracked longitudinally. Depending on the promoter used, the expression of the reporter gene can be restricted to a specific cell type or can be expressed constitutively. Many strategies have been developed, including enzymes, receptors, and iron-chelating proteins. While these approaches can provide information about the viability of the grafted cells and allows longitudinal tracking, epigenetic silencing or an immunogenic response by the host can occur [19]. Therefore, it is important that the signal or contrast is retained in the grafted cells or daughter cells.

Imaging modalities for cell tracking

In vivo cell tracking prefers noninvasive imaging modalities, such as PET, CT, SPECT, US, BLI, FLI, and MRI. For each imaging modality, accumulation and amplification of a specific signal from the contrast materials in the cells make it possible to localize, track and quantify the cell grafts. The source of the signal and contrast,

Table 2. Characteristics of imaging modalities

Imaging modality	*Spectrum*	*Probe/reporter used*	*Type of visualization*	*Spatial resolution*	*Temporal resolution*	*Signal depth*	*Longi-tudinal*	*In clinic*	*Cost*
SPECT	High-energy γ-rays	^{99m}Tc, ^{111}In, ^{123}I, NIS, NET	Whole-body	1~2 mm	min	Good	+	Yes	$$
PET	Low-energy γ-rays	^{18}F, ^{124}I, ^{64}Cu, HSV-tk, NET	Whole-body	1~2 mm	10 sec~min	Good	+++	Yes	$$$$
CT	X-rays	^{125}I, Gd	Whole-body	50~200 μm	min	Excellent	+	No	$$
US	High-frequency sound	Microbubbles, perfluorocarbons	Limited	1~2 mm	sec~min	mm~cm	+	No	$
BLI	Visible light	Luciferase	Whole-body*	3~5 mm, 3~5 μm*	min	1-2 cm	+++	No	$$
FLI	Near-infrared	QDs, Fluorescent proteins	Intravital microscope	3~5 mm, 2~3 μm*	sec~min	< 1 cm	++	No	$$
MRI	Radiowaves	Lanthanides, SPIO**, PEPE, Tyrosinase, β-galactosidase, LacZ, TFRC, FR, MagA	Whole-body	10~100 μm	min~hr	Excellent	+++	Yes	$$$
CEST-MRI	Radiowaves	HSV-tk, hPRM1, lanthanides, lipo-CEST	Whole-body	25~100 μm	min~hr	Excellent	+++	No	$$$

*non-*in vivo* or small animal only, **including USPIO, MION, CLIO. Abbreviations: NIS-sodium iodide symporter, NET-norepinephrine transporter, Gd-gadolinium, QD-quantum dots, SPIO-superparamagnetic iron oxide, PEPE-perfluoropolyether, TFRC-transferrin receptor, FR-ferritin, HSV-tk-herpes simplex virus type 1 thymidine kinase, hPRM1-human protamine-1.

acquisition techniques, and instrumentation differ from one imaging modality to the other. Therefore, each imaging modality has its advantages and disadvantages regarding sensitivity, spatial and temporal resolution, and imaging depth. A brief summary of the characteristics of different imaging modalities is presented in **Table 2**. With the rapid advances in imaging methods and imaging probes/reporters, the parameters given here are only applicable to the current state of each technology.

Single-photon emission computed tomography (SPECT)

SPECT is widely available in clinical diagnostic imaging. It detects the γ-ray signal emitted from radioactive isotopes with long half-lives ($t_{1/2}$), such as ^{99m}Tc, ^{111}In, and ^{123}I, using a rotating collimated gamma camera. The collected signal can be reconstructed as a 3-dimensional image. As a nuclear imaging method, SPECT has good sensitivity for imaging small numbers of cells with the ability to visualize up to 1×10^4 labeled cells with a temporal resolution of minutes [51]. Moreover, SPECT has shown improved resolution of labeled cells in an anatomical context. Although SPECT is not as sensitive as PET [52], the longer halftime of radiotracers is beneficial for the applications of cell labeling and cell tracking. One of the advantages of SPECT is that it allows multi-spectral imaging using multiple radionuclides (e.g. ^{111}In and ^{99m}TC [53]) simultaneously detecting multiple biologic events.

In recent years, reporter genes, such as enzymatic conversion/retention and receptor-mediated targeting, have been developed for cell tracking applications with SPECT. Sodium iodide symporter (NIS) can be imaged with ^{123}I or ^{99m}Tc for SPECT [54]. Norepinephrine transporter (NET), which can be labeled with ^{124}I-MIBG [55] as well as dopamine receptor and transporter, has also been used as a SPECT reporter [25]. These methods were applied to monitor neural stem cell [56] and cardiac stem cell [24] grafts, as well as to monitor neuronal differentiation [57].

While most studies reported no detrimental impact of isotopes used in SPECT imaging, one study found low labeling efficiency (32%), reduced viability, and complete impairment of proliferation and differentiation in CD34$^+$ hematopoietic progenitor cells [58]. Another study involving human mesenchymal stem cells (hMSC) demonstrated that ^{111}In-oxiquinolon affected cell migration [59]. One major concern in using SPECT for cell tracking is that radioisotopes exhibit substantial efflux within 24 hours [53]. For applications in longitudinal monitoring and follow-up studies, the emitted γ-rays are potentially mutagenic and carcinogenic.

Positron emission tomography (PET)

PET is another popular clinical and preclinical imaging modality. It offers the most sensitive method for tracking relatively scarce cells with extraordinary sensitivity in the picomolar range (10^{-11}-10^{-12} mol/l) [60, 61]. The signal for PET is produced from positron-emitting radionuclides, such as ^{11}C, ^{13}N, ^{18}F, ^{124}I, and ^{89}Zr [52, 62]. Upon the annihilation of a positron, the emission of two anti-parallel γ photons is detected by a sensitive photodetector. The signal is later computed for a spatial position with the intensity of the emission sources. Direct labeling and genetic reporter systems for tracking cells with PET have both been explored recently. In a recent study, mouse embryonic stem cells were labeled with widely available fludeoxyglucose ([^{18}F]-FDG) to monitor retention of grafted cells *in vivo* [63]. Monitoring of neural stem cell migration has been reported with 3'-deoxy-3'-[^{18}F]fluoro-L-thymidine [64].

Reporter gene and reporter probe paradigms have also been developed for PET. Herpes simplex virus type 1 thymidine kinase (HSV-tk) and probe (2'-fluoro-2'-deoxy-l-)3-D-arabinofuranosyl-5-iodouracil (FIAU) have been evaluated for myocardial gene therapy in pigs [65]. In addition to HSV-tk and FIAU, gene reporter and probe pairs, human sodium iodide symporter (NIS) with ^{124}I and human estrogen receptor ligand binding domain (hERL) with 16α-[^{18}F] fluoro-17β-estradiol (^{18}F-FES) have been evaluated for *in vivo* tracking of hMSC grafts in mouse [66, 67].

However, applications of PET imaging are often limited by its substantial requirement in resource setup and complexity in the development of new tracers. Since it is a nuclear imaging method, there is a concern of possible mutagenic and carcinogenic effects of high energy γ photons. Comparing to MRI, another widely available clinically translatable cell track-

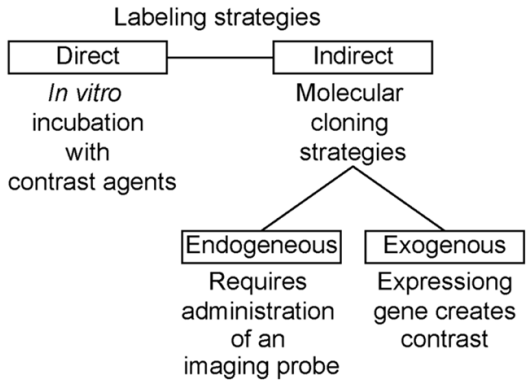

Figure 2. Different labeling strategies highlighting the main differences among different strategies.

ing imaging modality, PET does not have as high a spatial resolution [61].

Bioluminescence imaging (BLI)

Bioluminescence imaging is one of the preclinical optical imaging methods that use luminescent light (peak wavelength ~450-600 nm) emitted from a product of an enzyme-mediated chemical reaction, i.e., luciferin oxidized by the enzyme luciferase in the presence of ATP and oxygen [68, 69]. Genetic reporter luciferase and BLI are the most established and popular cell tracking imaging approach in rodent studies. For *in vivo* BLI imaging, animals are placed in a dark chamber with a sensitive photodetector, and D-luciferin is needed to be injected shortly before imaging. The emitted light is often detected by a charge-coupled device (CCD) camera. Among many luciferases identified and cloned, there are two isolated from two different organisms that are commonly employed: firefly (*Photinus pyralis*) and sea pansy (*Renilla reniformis*). Due to its structural and auto-oxidation properties, the luciferase isolated from the firefly is more broadly used for *in vivo* tracking. The feasibility of BLI relies basically on the ability to establish the cell lines that can incorporate and stably express the luciferase report gene for longitudinal monitoring [28]. BLI has made a great impact in the field of molecular and cellular imaging and continues to be one of the mostly applied imaging tools in preclinical studies, including cell tracking research. In a recent study, human neural progenitor cells (NPC) grafted in mouse brain was tracked *in vivo* for 12 weeks [29]. Also, the aforementioned study by Wolfs et al. [66] used BLI as one of the imaging modalities for their multimodal imaging of hMSC. BLI was also used to evaluate the engraftment efficiency, proliferation, and therapeutic potential of iPSC-derived cardiomyocytes in a mouse myocardial infarction model [70].

However, as an optical imaging method, the poor signal penetration and imaging depth limit the use of BLI mostly to rodents [40]. Since the wavelength used in typical BLI is 400-700 nm, the signal is highly susceptible to absorption and scattering in living tissue [40]. Even in mice, background signal can cause false-negative findings [71]. Also, the pharmacokinetics of luciferin has to be taken into account since each organ has a different absorption rate, catalysis rate, and elimination kinetics for luciferin [72]. Moreover, BLI requires injection of the high concentration of substrate compounds that are potentially immunogenic substances unlikely to be used in human [40].

Fluorescence imaging (FLI)

Unlike BLI using mostly genetic imaging reporter, FLI uses mostly organic/inorganic fluorophores (e.g., quantum dots) for labeling the cells but also can use genetically introduced reporters (e.g., green fluorescent protein, near-infrared fluorescent protein) [31]. The signal is produced by the fluorescence molecule when the molecule is excited by a specific incident wavelength and emits back light [31]. For *in vivo* monitoring of grafted cells, near-infrared (650-900 nm) fluorescent synthetic molecules and nanoparticles as well as near-infrared proteins, have shown great promise due to the relatively better signal penetration up to 10 mm comparing to other fluorescent light [32].

Comparing to BLI, FLI shows broad applications in preclinical studies given more choices of fluorescent probes available. For whole-body imaging, FLI suffers from the same limitations as BLI such as light scattering and signal absorption by surrounding tissue, which limits the depth of tissue to only the surface area. Even with tomographic imaging methods, spatial resolution is limited to approximately 1 mm [73]. However, the cytotoxicity, impact on host cell differentiation, signal penetrance, and light-scattering characteristics of such reporter need to be investigated.

Table 3. Lists of direct and indirect probes/reporter

Probing method	Probe/reporter	Imaging modality	Toxicity reported	Research area	FDA approved
Direct	Gd^{3+} [149] or Mn^{2+} [150]	MRI-T_1 (+)	Yes	Viability, migration	Yes
	SPIO [151, 152], USPIO [153], CLIO [154], MION [155]	MRI-T_2 (-)	Yes	Viability, migration	Yes
	PFC [156, 157]	^{19}F MRI	Yes	Viability, migration	Yes
	QD [158]	FLI	Yes	Immunology (homing)	Yes
	Fluorescent probe [159]	Intravital microscope	No	Migration, cell-cell interaction, infiltration, homing	Yes
	^{111}In [51], ^{99m}Tc [53]	SPECT	Yes	Homing, cell therapy efficacy	Yes
	^{18}F [64], ^{64}Cu [160]	PET	Yes	Homing	Yes
Indirect	Ferritin/transferrin receptor [35, 161]	MRI-T_2/T_2* (-)	No	Viability, migration, differentiation	No
	β-galactosidase [79]	MRI-T_1/T_2/T_2* (-)	Yes	Viability, migration	No
	Tyrosinase [23]	MRI-T_1 (-)	Yes	Viability	No
	MagA [37, 38, 116, 117, 119]	MRI-T_2/T_2* (-)	No	Viability	No
	Plasma membrane bound reporter peptide [162]	MRI-T_1/T_2/T_2* (+/-)	Yes/No	Viability, differentiation	No
	Lysine-rich protein [131]	CEST	No	Viability, migration, pH sensing	No
	Fluorescent protein [163]	FLI	No	Migration, cell-cell interaction, infiltration, homing	No
	Luciferase [29, 57, 163]	BLI	No	Migration	No
	HSV-tk (^{18}F) [65, 66]	PET/SPECT	Yes	Viability, migration	No
	NET [55]	PET/SPECT	Yes	Migration, homing	No
	NIS [56, 66]	SPECT	Yes	Migration, homing	No
	Dopamine 2 [164]	PET	Yes	Viability	No
	Somatostatin [165]	PET/SPECT	Yes	Viability	No
	DMT1 [100]	MRI-T_1 (+)	No	Viability	No

For MRI- (-) for negative contrast and (+) for positive contrast. Abbreviations: MION-monocrystalline iron oxide, USPIO-ultrasmall superparamagnetic iron oxide, CLIO-cross-linked iron oxide, PFC-perfluorocarbon, PEPE-perfluoropolyether, SPIO-superparamagnetic iron oxide, NIS-sodium iodide symporter, NET-norepinephrine transporter, QD-quantum dots, DMT1-Divalent metal transporter 1.

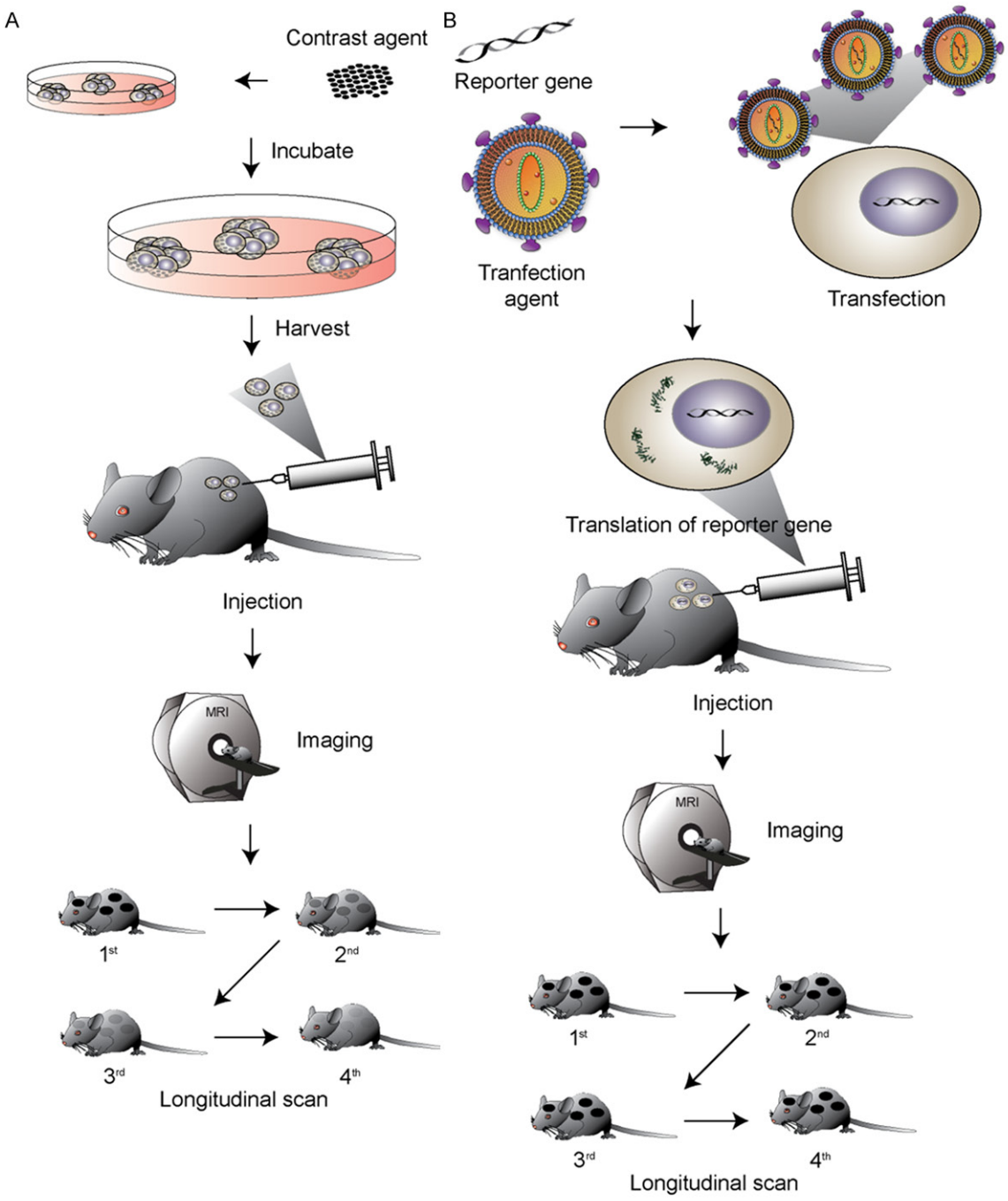

Figure 3. Direct and indirect labeling methods. A. In the direct labeling method, cells are incubated with a contrast agent (e.g. SPIO). Cells actively take up the contrast agent and are harvested after a specific incubation period. The harvested cells are injected into a study subject, and the cells are tracked using the imaging modality of choice. The major limitation of the direct labeling method is the dilution of contrast agent. B. For the indirect labeling method, a reporter gene is transduced into the cells, and cells expressing the reporter gene are injected into a study subject. The major advantage of the indirect labeling method is that the contrast agent does not get diluted by cell division, allowing longitudinal monitoring.

Computed tomography (CT)

X-ray CT is the most available and affordable imaging modality. Yet, CT fell out of favor as an imaging modality for stem cell tracking because it has less soft tissue contrast for studying the soft tissue organs, and may require the use of a high concentration of high-density/high-atom-

ic-number materials as contrast agents [40]. However, with the recent development of multi-imaging modality methods, CT has been used to track MSC grafts in rabbits [74].

Ultrasound (US)

The contrast for ultrasound is achieved by acoustic interfaces (e.g. microbubbles and perfluorocarbons) [40]. The advantages of ultrasound include low-cost, wide availability in most clinics and lack of long-term side effects. However, ultrasound has various limitations for cell tracking, such as poor anatomic coverage (unable to performing whole body imaging), limited contrast materials, the acoustic "shadowing" effect and limited signal penetrance depth [27]. Despite these limitations, US has been used in prostate stem cell monitoring with nanotubes [75] and *in vivo* neural progenitor cell tracking with microbubbles [26].

Magnetic resonance imaging (MRI)

Magnetic resonance imaging is a widely available clinical and preclinical imaging modality offering a superior spatial resolution, 3-dimensional imaging capability, and high soft tissue contrast for non-invasive *in vivo* tracking of cell grafts. Compare to SPECT and PET, MRI does not require the use of radioactive isotopes. Due to these advantages, MRI has become the most attractive imaging modality for tracking stem cells *in vivo* (**Figure 1B**).

Most commonly used MRI detects the signal that originates from mobile water protons (^{1}H) but it can be also used for tracking cells labeled with fluorinated molecules (^{19}F) or other nuclei if sensitivity is sufficient. The contrast for MRI is typically generated by either manipulating pulse sequences to exploit differences in relaxation properties of water protons or introducing contrast agents (e.g., Gd^{3+} or iron oxide) that alter the relaxation properties of water protons in the region where contrast agents accumulate. When the external magnetic field is removed, magnetic moments re-align in the external magnetic field direction (B_0). The time it takes to recover net magnetization is called longitudinal relaxation time or spin-lattice (T_1) relaxation. The conventional MRI measures the relaxation of protons. The T_1 relaxation time depends on the mobility of the proton (spin-lattice) or the gyromagnetic ratio of the nucleus.

On the other hand, transverse relaxation time (T_2) describes the diminishing net transverse magnetization or the loss of spin coherence by dephasing of spins. MRI contrast agents are those paramagnetic materials that can accelerate the relaxation times of the protons affected, inducing either T_1 or T_2 relaxation of juxtapositioned protons generating hyper- or hypointense signal. T_1 contrast agents, such as lanthanide chelate Gd-DTPA, typically generates the hypointense signal from those water molecules recovered fast than background due to the presence of the contrast materials. The T_2 contrast agent, such as iron oxide nanoparticles, cause net transverse magnetization or signals diminishing fast under the effect of the contrast agents the, generating hypointense or "dark" contrast due to signal drop. Two factors affect T_2 relaxation: molecular interactions and local magnetic field inhomogeneity. Combinations of these artifacts result in hastened decay of transverse magnetization, referred to as T_2*.

Labeling cells for MRI tracking: There are two methods to label cells: direct and indirect (**Figure 2**, **Table 3**). The direct labeling method (**Figure 3A**) takes advantages of cell endocytosis of a contrast agent (e.g. SPIO) [149-160]. Stem cells are incubated in culture conditions with the contrast agent which can be taken up by the cells. The contrast agent can be surface modified with cell membrane receptors to enhance cellular uptake. Although the direct labeling method is relatively easy to employ, there are several limitations when used in cell tracking and longitudinal monitoring *in vivo*. First, the labeling agent is diluted as cells divide, and such dilution limits the duration of monitoring. Second, the contrast agent can be released from apoptotic cells and taken up by adjacent cells (i.e. false-positive signal) or even localize to the extracellular matrix. The first and second limitations of the direct labeling method were well demonstrated in a study involving tracking of *lacZ* expressing neural stem cells labeled with SPIO [76]. In this study, the rapid division of neural stem cell grafts resulted in the dilution of MRI contrast. In postmortem analysis, they further demonstrated a lack of MRI contrast in the stem cell-derived neuronal cell populations [76]. When transfection agents are sometimes used to assist the cellular uptake of the labeling agent, they can affect

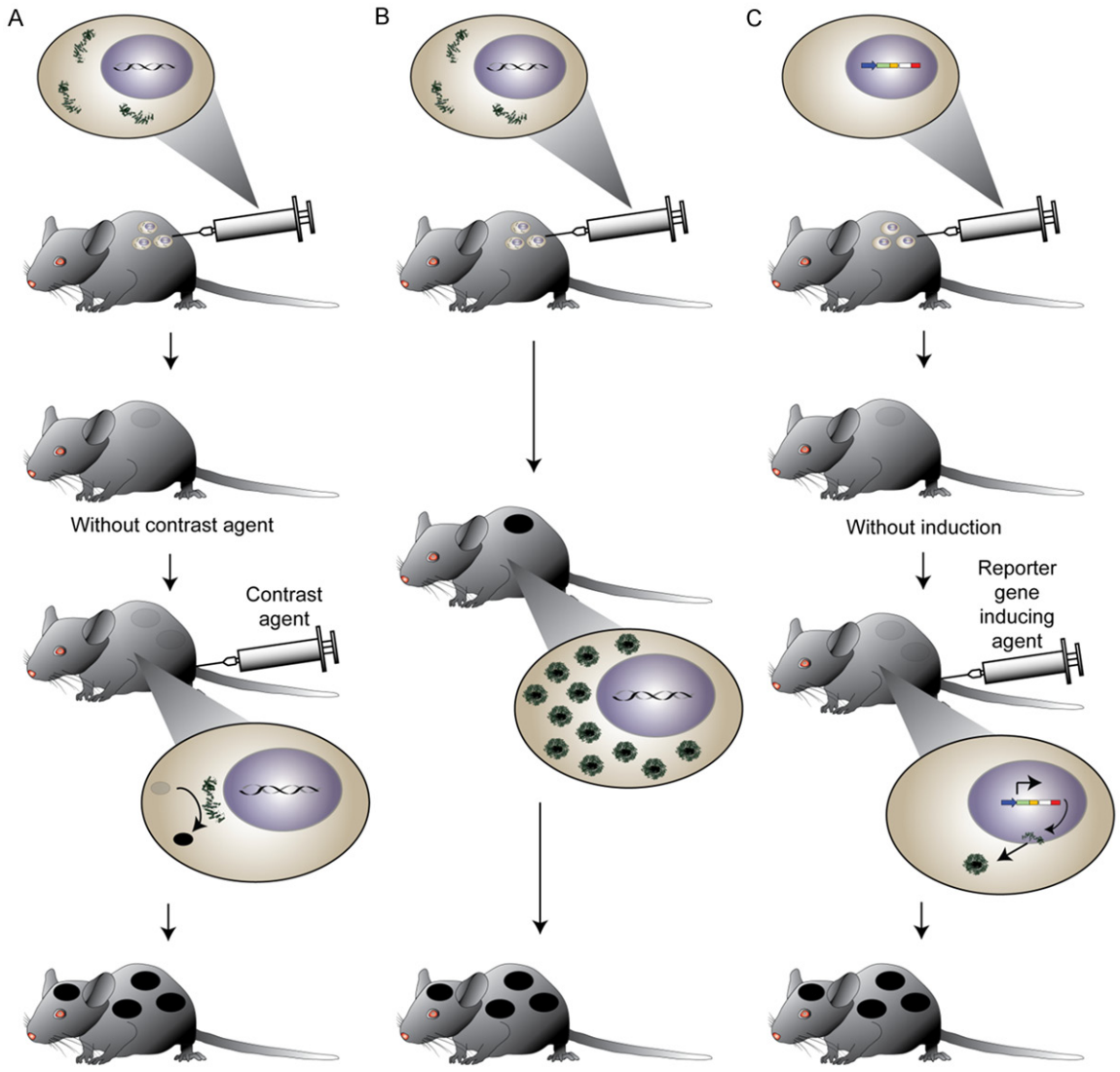

Figure 4. Exogenous and endogenous labeling methods. A. Exogenous labeling methods require injection of a contrast agent. Either binding of the contrast agent or activation by enzyme generates contrast. B, C. Endogenous labeling methods. B. The constitutive expression does not require injection of contrast agent but lacks the mechanism to regulate the expression. C. An inducible promoter allows expression of the reporter gene when monitoring is required.

the motility, differentiation potential, viability, proliferation, and functionality [77].

To address these limitations, the indirect labeling method (**Figure 3B**) employing molecular cloning strategies to produce endogenous MRI contrast materials, such as iron chelating or storing proteins intracellularly, or specific cell targets for MRI contrast probes, has been explored [161-165]. The indirect labeling method can be further divided into exogenous (reporter mediated) and endogenous (*de novo*) methods (**Figure 4**) [17, 18]. The exogenous method requires administration of an imaging probe (**Figure 4A**). One limitation of the exogenous labeling approach is that the sufficient delivery of the probe for high contrast and sensitivity highly depends on the targeted accumulation and pharmacokinetics of the imaging probe [18]. In contrast, the endogenous method (**Figure 4B**) depends on developing and engineering a proper gene construct for a genetic imaging reporter. The endogenous reporters, however, have limited MRI contrast.

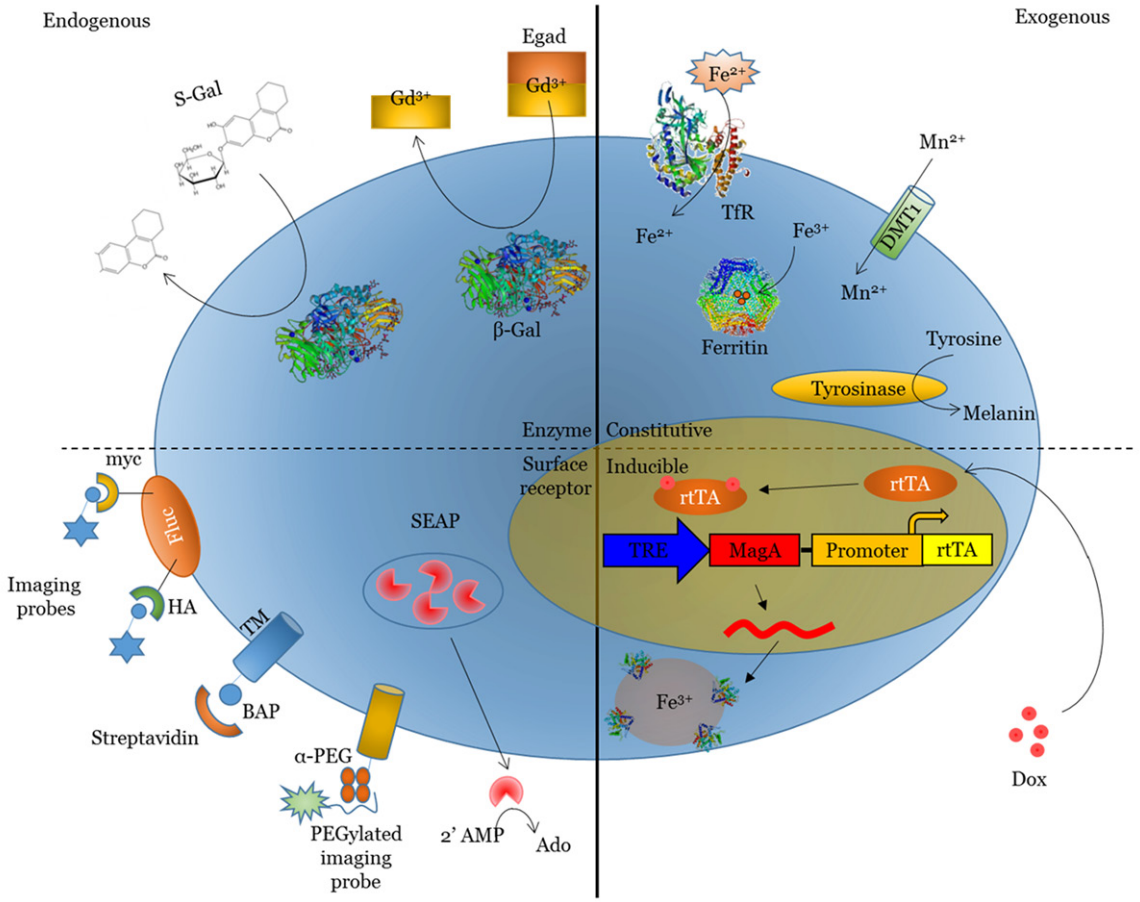

Figure 5. Exogenous and endogenous genetic reporters.

There is also concern that a continuous expression of the reporter gene can result in unforeseen consequences including cytotoxicity. In one study, chronic overexpression of H-ferritin (FTH1) resulted in a neurodegeneration phenotype [78]. Ideally, the expression of a reporter gene could be regulated by an inducible promoter, such as Tet-On or Tet-Off switches (**Figure 4C**). The controllable expression approach adds safety by minimizing the impact (on proliferation, migration, and differentiation) of constitutive expression of the reporter. However, both exogenous and endogenous methods share some limitations that include low dynamic resolution because the lifetime of the signal depends on the clearance of the reporter and genetic manipulation of stem cells is required, making clinical application unlikely.

Exogenous MRI reporters: There are two types of exogenous reporters to date: enzymes and engineered cell surface peptides (**Figure 5**). The first exogenous MRI reporter gene was reported in 1997 [79]. In this study, a molecule, Egad, was synthesized containing gadolinium (III), Gd^{3+}, in a cage composed of galactopyranose ring and tetraazamacrocycle. When the molecule was exposed to β-Galactosidase, galactopyranose was removed from the molecule, and the exposure of Gd^{3+} enhanced longitudinal relaxation of water molecules, resulting in positive T_1 contrast [79]. A contrast agent containing gadolinium, gadopentetate dimeglumine, was the first FDA-approved MRI contrast agent [80]. Gadolinium has been used to track mesenchymal stem cells [81], hematopoietic progenitor cells [82], and endothelial progenitor cells [83]. However, it has been reported that gadolinium could induce nephrogenic systemic fibrosis and even death [84]. Manganese (Mn^{2+}) is another T_1 contrast agent with positive contrast. A recent study used silica-coated manganese oxide (MnO) nanoparticles to track mesenchymal stem cells [85]. The *lacZ*/β-

galactosidase system has the versatility of providing T_1, T_2, or T_2* contrast depending on the contrast materials used as the probe. It has been demonstrated that β-galactosidase expressing MSC can be tracked *in vivo* by S-Gal™ as an imaging probe, which enhanced T_2 and T_2* MR contrast [86]; yet several limitations were observed for the *lacZ/β-galactosidase* system, including the efficient delivery of the probe which depends on the pharmacokinetics of the probe, the limited uptake of the probes by the targeted cells as probe concentration diluted rapidly once injected, the nonspecific cellular uptake of the injected imaging contrast agent, and the possible effects on cell viability [17]. Superparamagnetic iron oxide particles (SPIOs) offer ultrahigh T_2 relaxivity hence produce greater sensitivity, which make it optimal to track a small number of cells such as neural cells [87]. Since non-phagocytic cells do not internalize the SPIO nanoparticles, an alternative approach is used to engineered cell surface peptides. An engineered surface protein expressing hemagglutinin (HA), luciferase, and myelocytomatosis (myc) (i.e. HA-fluc-myc) was developed as an MRI reporter [88]. HA and myc serve as the molecular target for antibody conjugated with SPIO. Both human and mouse ESCs expressing HA-fluc-myc have shown significant hypointense signal in proliferating ESCs and teratoma [88]. Other surface receptors, such as a biotinylated transmembrane receptor (BAP-TM) and anti-polyethylene glycol (PEG) peptide, have also been developed as genetic MRI reporters and could be detected in cancer cells [89, 90]. In a few early clinical trial studies, SPIO nanoparticles were used to track homing of mesenchymal stem cells to central nerve systems in individuals with multiple sclerosis and amyotrophic lateral sclerosis [91]. Also, Ferumoxytol®, an FDA approved ultrasmall superparamagnetic iron oxide nanoparticles (USPIOs) used as an iron supplement for treating anemia, was used to label and track human neural stem cells in mouse brain [92]. In 2010, Westmeyer et al. developed an interesting method using a secreted enzyme as a genetic MRI reporter. This study revealed that secreted alkaline phosphatase (SEAP) could be used as a genetic MRI reporter as it promotes aggregation of SPIO [93]. Most recently, 'hot spot' highly shifted proton (HSP) MRI reporter was developed [94]. The tumor cells were labeled with dysprosium (Dy)- or thulium (Tm)- 1,4,7,10-tetraazacyclododecane-1,4,7,10-tetramethy-1,4,7,10-tetraacetic acid (DOTMA) and was imaged by the ultra-short echo time (UTE) sequence. Dramatically shortened T_1 contrast could be demonstrated [94]. This method has a detection limit of about 1×10^4 cells [94].

Endogenous MRI reporters: Endogenous MRI reporters use a gene or set of genes that do not require exogenous substrates to generate MRI contrast. The first reported endogenous MRI reporter was transferrin receptor (*Tfrc*) [33]. When Tfrc was overexpressed in cells, R_2* contrast was significantly enhanced [33]. Later, there was improved contrast when transferrin-associated SPIO was used, which takes advantage of an endogenous approach with the exogenous approach [95]. Although iron is crucial for normal cell function, internal free labile iron is strictly maintained by networks of genes [96]. Other genes involved in iron homeostasis, like transferrin (*Trf*) and ferritin, have also been explored. Transferrin is involved in transporting iron into the cell while ferritin is involved in storing iron in the cell. Of all the genes involved in iron homeostasis, ferritin has proved to be the most popular [17]. The overexpression of a heavy chain of ferritin (FTH1) is found to generate T_1 and T_2 contrast *in vitro* and *in vivo* [34]. One study has expressed human FTH1 as a reporter for *in vivo* tracking of cardiac stem cells [97]. Cell survival was monitored up to 4 weeks after grafting using T_2-weighted imaging and T_2* mapping [97]. To demonstrate the sensitivity of the system, human FTH1 and Tfrc were also coupled and overexpressed in murine neural stem cells. The overexpression resulted in enhanced transverse relaxivities observed in both R_2 (i.e., $1/T_1$) and R_2* (i.e., $1/T_2$*) [97]. Ten days after the graft, T_2*-weighted imaging yielded increased contrast only with 2,500 cells [97]. FTH1 has been used for stem cell tracking, such as in embryonic stem cells [35] and myoblasts [98]. These studies have shown significant MR signal enhancement between 14 to 21 days after injection. However, further investigation is needed to assess the impact of overexpressing FTH1 on iron homeostasis in different cell types. The overexpression of Tfrc is known to activate iron overload response, and the overexpression of FTH1 or FTL1 activates iron deficiency response [18].

In 1997, another endogenous MRI reporter gene, tyrosinase, was reported [99]. Tyrosinase is the primary enzyme involved in melanin pro-

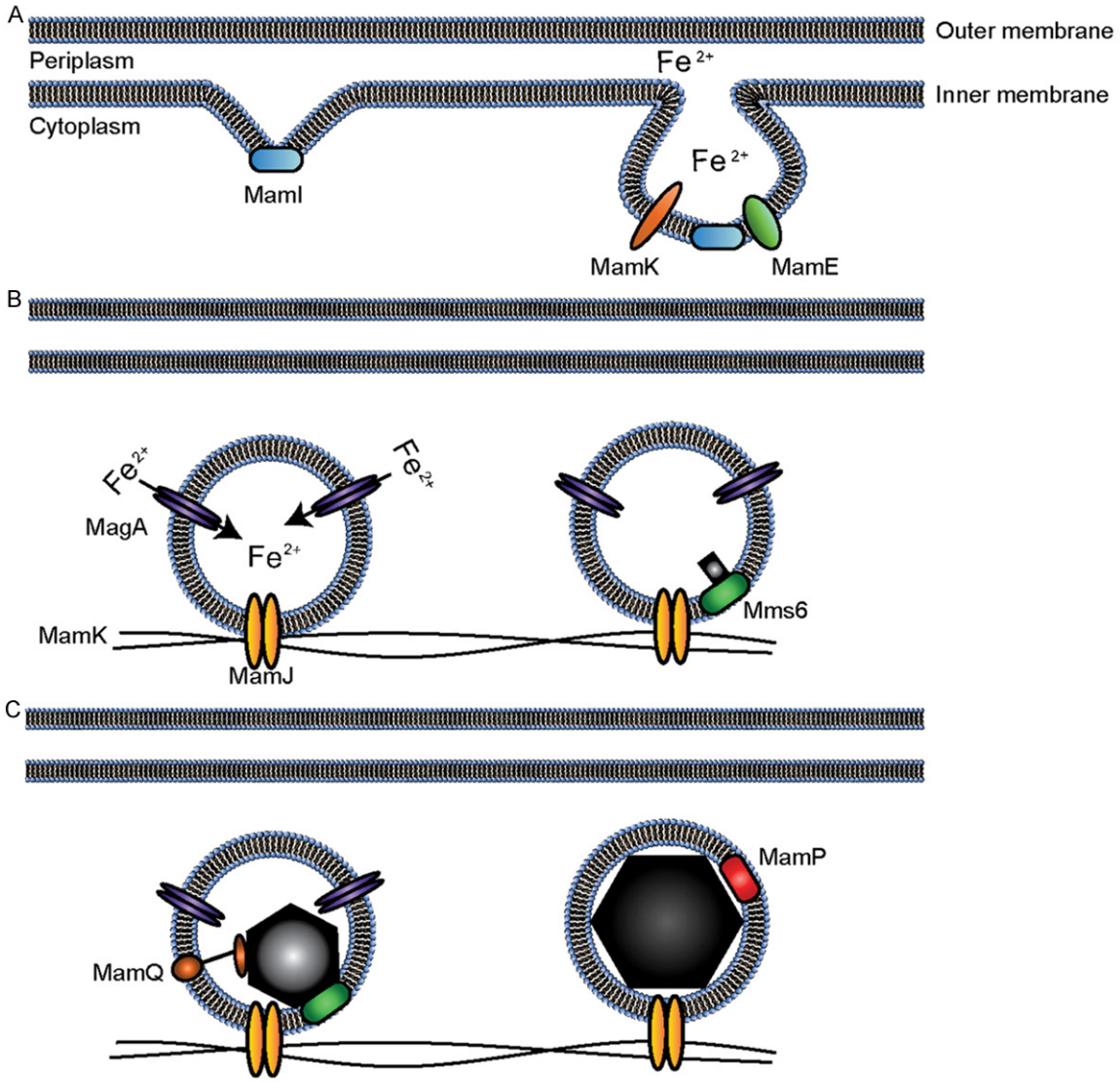

Figure 6. A current model of the magnetosome formation process. A. The first step of magnetosome formation is invagination and vesicle formation. The initial invagination process is activated by MamI, L, Q, and B. A vesicle is formed by recruiting additional proteins (e.g. MamK and E). B. After the vesicles are formed, they are aligned on a chain via interaction between MamK, cytoskeletal structure, and MamJ, a membrane-bound protein. Mm6 is involved in the biomineralization process. C. A magnetite crystal starts to form with an increase of iron content in the vesicle, with many proteins involved in the process (i.e. MamA, G, F, D, and C). MamP appears to be involved in the size restriction.

duction, and the overexpression of tyrosinase results in melanin accumulation. Melanin is excellent at sequestering paramagnetic ions, which results in T_1 contrast [99]. Although tyrosinase has not been used in stem cells, interest in using tyrosinase as an MRI reporter has risen due to its ability to be employed in multimodal imaging, combining MRI, photoacoustic, and PET [23].

A divalent metal transporter-1 (DMT1) was tested as a novel MRI reporter gene. The overexpression of DMT1 enhanced manganese uptake and resulted in a significant increase in R_1 [100]. Unlike hypointense contrast caused by the attenuation of MR signal with iron homeostasis associated genes, DMT1 resulted in hyperintense contrast with signal enhancement, which was correlated with better sensitivity. However, intraperitoneal injection of $MnCl_2$ was needed to achieve better contrast. Also, the systemic and cellular impact of exposure to manganese must be further investigated.

Table 4. Magnetosome-associated genes

Gene name	Essential	Process involved
magA [110], feoB [104]	Somewhat [105]	Iron transporter
chpA [109]	Yes [105]	Copper-dependent, high-affinity iron transporter
mamB, M [166]	Yes [105]	Biomineralization and membrane assembly
mamH [167], N [103]	No [105]	Major facilitator superfamily of transporter
nir [168] l, nap [169]	Yes [105]	Reduction of nitrate to nitric oxide (oxidizing ferrous iron)
mamE, P, T [170], O [103]	Yes [105]	Magnetochrome/electron transport chain
mamX [167]	No [105]	Magnetochrome/electron transport chain/iron reductase
mamZ [167]	No [105]	Iron reductase
mms6 [106]	No [105]	Regulation of the mineralization of iron
mad25, 23, 10, 11, 12 [107]	No [105]	Shape and size regulation of biomineralization
mamG, F, D, C [171]	No [171]	Biomineralization/regulates size of the magnetite crystal
mamQ [172]	Yes [105]	Biomineralization
mamJ, K [172]	Yes [105]	Cytoskeletal structure
mamI, L [172]	Yes [105]	Vesicle formation

Another possible endogenous MRI reporter candidates are the genes involved in magnetosome formation in bacteria. Magnetosome is a magnetite-enriched organelle. Magnetite crystals are considered to be an excellent MRI contrast agent because they can drastically shorten transverse relaxation time (T_2 and T_2*). The biosynthesis of magnetosomes was achieved in non-magnetosome-forming bacteria by an elaborate stepwise recombination method, which elucidated the genes responsible for magnetosome formation [101]. Magnetite nanocrystals are considered to be superparamagnetic, with much greater magnetic susceptibility than the paramagnets. Superparamagnetic iron oxide nanocrystals may form in mammalian cells through biosynthesis of magnetosomes while protecting the host cell by isolating magnetite in membrane-bounded magnetosome organelles (**Figure 6**) [52]. The formation of magnetosome starts with invagination of the inner plasma membrane. The newly formed vesicle is attached to the cytoskeletal structure in the cell. Next, iron is actively transported into the vesicle. Lastly, the iron in the vesicle is actively incorporated into the magnetite crystal, and the shapes and sizes of the crystals are determined by the specific species [102]. However, the lack of mammalian homologs of genes involved in magnetosome formation could lead to immune reactions. The formation of the magnetosome is controlled by a set of proteins with specific biological functions. These proteins are unique to magnetotactic bacteria (MTB) and are encoded by genes identified by genomic comparison of four species of MTB with nonmagnetotactic bacteria [103]. Among 28 genes identified, 18 were located within the magnetosome genomic island (MAI). There are some operons in the MAI: magnetosome membrane (Mam), magnetic particle membrane specific (Mms), and a monocistronic MamW [104]. Also, there are operons outside of the MAI, and these are magnetotaxis (Mtx) and magnetosome membrane (Mme) [102]. The functions of several operons are still under investigation. Some of these operons have an apparent association with the biosynthesis of magnetosomes while others have little or no association. Genes that are associated with magnetosome formation are listed in **Table 4** with their putative functions [166-172]. In *Magnetospirillum magneticum* (strain AMB-1), only the genes in the mamAB operon are found to be essential for magnetosome formation [105]. The genes involved in biomineralization and iron transport are particularly interesting from the MR imaging perspective. There are a number of genes found to be involved in biomineralization: *mms6*, *mad* (*10, 11, 12, 23, 25*), and *mam* (*G, F, D, C*). Of these, *mms6,* identified in magnetite crystals, has been studied extensively [106]. *mms6* regulates the mineralization of magnetites by binding to iron on the C-terminal domain [107]. Recently, a study reported using *mms6* as an MRI reporter leading to a significant increase in R_2 and offering potential promise for *in vivo*

Table 5. *magA* homology BLAST search result

Gene	Organism	Function	Max score	Identity
Na^+/H^+ exchanger	Magnetospirillum gryphiswaldense	Sodium/hydrogen exchanger	544	69%
Kef-type K^+ transport system	Caenispirillum salinarum	K^+ transporter	402	55%
Ferrous transporter	Candidatus Odyssella thessalonicensis	Fe^{2+} transporter	305	44%
Na^+/H^+ antiporter/ferrous transporter	Nitratireductor indicus	Sodium/hydrogen exchanger and ferrous transporter	304	44%
Na^+/H^+ antiporter/ferrous transporter	Fulvimarina pelagi	Sodium/hydrogen exchanger and ferrous transporter	254	40%
CPA2	Glaciecola chathamensis	monovalent cation/H^+ antiporter	217	38%
Na^+/H^+ exchanger	Mariprofundus ferrooxydans	Sodium/hydrogen exchanger	206	35%
KefC	Francisella sp.	Glutathione-regulated potassium-efflux	214	31%
KefB	Nitritalea halalkaliphila	Potassium transporter	189	31%

Table 6. MagA conserved domain

Conserved domain	
TM PBP1	Transmembrane subunit of periplasmic binding protein (PBP)-dependent ATP-Binding Cassette (ABC) transporters
Na^+/H^+ exchanger	Sodium/hydrogen exchanger superfamily
KefC	Kef-type K^+ transport system (inorganic ion transport and metabolism)
2a37	Transporter, monovalent cation/proton antiporter-2 (CPA2) family-transport and binding proteins, cations and iron-carrying compounds
RosB	Kef-type K^+ transport system, predicted NAD-binding component (inorganic ion transport and metabolism)
KefB	Kef-type K^+ system, membrane component (inorganic ion transport and metabolism)
NhaP	NhaP-type Na^+/H^+ and K^+/H^+ antiporters (inorganic ion transport and metabolism)

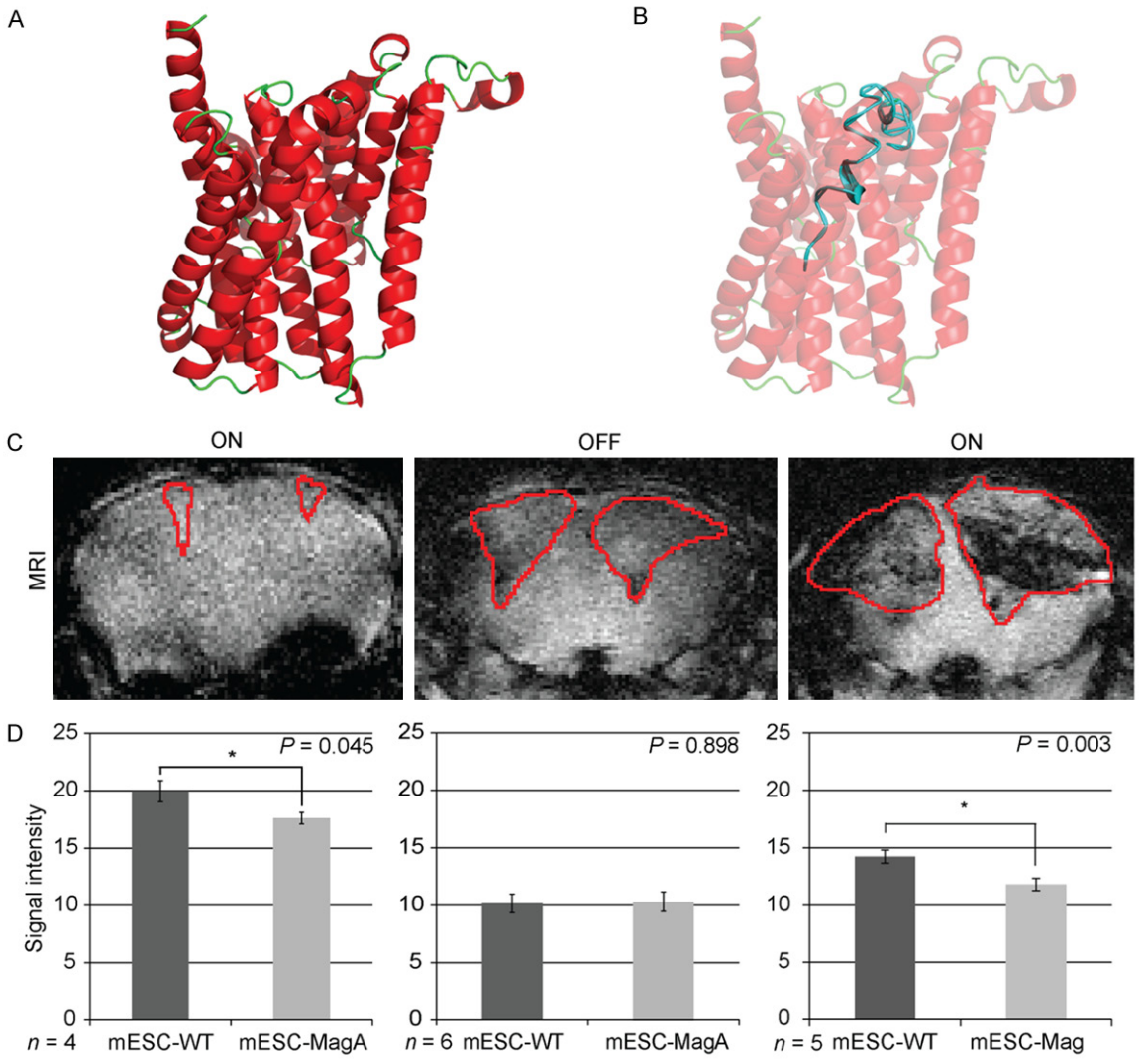

Figure 7. MagA structure and longitudinal monitoring of stem cell graft using inducible MagA as a genetic MRI reporter. A. Phyre server-generated MagA 3D structure. B. Superimposed model of MagA and c2k3ca. C. A representative MRI image of a single mouse, with the status of MagA expression at the top of images. MRI images were taken in a 7-day interval. D. Regions of interest (ROIs) analysis of signal intensity showing significant hypointense signal with the "On" states, while no such difference was observed for the "Off" state [119].

tracking of tumor cell grafts [108]. However, the efficacy of *mm6* in stem cell graft tracking regarding its impact on toxicity, proliferation, differentiation, and migration still need to be evaluated. If *mms6* is similar to a ferritin system (iron chelator), *magA* and *chapA* act more like a transferrin receptor. When overexpressed, iron transporters might increase the iron content of the cell, allowing the cell to be monitored using MRI. For these reasons, *chapA* and *magA* have been investigated as MRI reporters. MagA is a membrane iron transporter protein involved in magnetosome formation in magnetotactic bacteria [109-111]. *magA* is homologous to Na^+/H^+ transporter, ferrous transporter, CPA2, KefC, and KefB (**Table 5**) [112]. A member of KefB superfamily, 2a37, protein domain is highly conserved in MagA (**Table 6**). KefB is a glutathione-regulated potassium efflux system [113] with a metal-binding domain (**Figure 7A**, **7B**) [114, 115], which suggests that MagA is a membrane protein with possible metal transportability. The MagA predicted model and c2k3ca (metal transporter templates) were aligned to create a superposition model to illustrate a possible iron-binding domain (**Figure 7B**). Although the complete reconstruction of a magnetosome in foreign cells has not been

achieved, a number of studies have found that the overexpression of MagA increased MRI contrast [37, 38, 116, 117].

Compared to the constitutive expression of an MRI reporter gene, an inducible system can have several advantages. First, controllable expression of an MRI reporter can minimize the adverse effects of constitutive expression of a reporter gene (e.g. toxicity, reduced proliferation rate, possible impact on differentiation potential). Another advantage is the use of an inducing agent with well-documented pharmacokinetics. One of the agents, doxycycline, has been widely used in controllable expression systems and has shown low toxicity and the ability to cross the blood-brain barrier, as well as the placenta barrier [118]. Inducible MRI reporters have been reported in *in vivo* monitoring of cell grafts. Cohen et al. have achieved *in vivo* monitoring of C6 glioma tumors expressing TET-EGFP-HA-ferritin [34]. By employing the Tet-Off system, they were able to illustrate that the overexpression of murine FTH resulted in significant R_2 relaxation up to 28 days post-transplantation [34]. Zurkiya et al. demonstrated the efficacy of monitoring tetracycline-inducible (Tet-On) MagA in human embryonic kidney cells (293FT) transplanted in the striatum of mice [37]. Tet-On MagA was also used for repetitive longitudinal monitoring of intracranial mouse embryonic stem cell (mESC) grafts *in vivo* [119]. This study took advantage of both the MagA system and inducible Tet-On system to regulate reporter expression and demonstrated repetitive monitoring correlation to the status of reporter expression [119].

Another genetic MRI reporter, ferritin, has also shown the efficacy of using an inducible promoter. Nasopharyngeal carcinoma cells expressing human ferritin heavy chain (FTH1) under the regulation of the Tet-Off system were used for *in vivo* monitoring of cell grafts [120]. Feng et al. observed a significant increase in transverse relaxivity (R_2) with the overexpression of FTH1. The proliferation, cytotoxicity, apoptosis, and migration of the cell could be assessed. The induction of gene expression in a cell graft was also detected by the genetic MRI reporter. In 2007, Cohen et al. generated transgenic mice with the TET:EGFP-HA-ferritin (tet-hfer) transgene [121]. By mating with mice expressing the tetracycline transactivator (tTA) under a tissue-specific promoter (e.g. vascular endothelial (VE) cadherin promoter and liver activator protein (LAP) promoter), expression of the tissue-specific genes was monitored with MRI [121]. In a more recent study, Rohani et al. compared the ability of MagA and FTH1+FTL1 to enhance the MR contrast *in vivo*. Here, MagA or FTH1+FTL1 lacking iron response element was expressed in human breast/melanoma (MDA-MB-435) cells and used for repetitive imaging of a tumor. MagA expression resulted in similar contrast to FTH1-FTL1-expressing cells and exhibited contrast enhancement up to 20 days [38]. Also, the same group was able to present similar results *in vitro* showing similar contrast from the cells expressing either MagA or FTH+FTL1 [117]. In our lab, we have demonstrated longitudinal and inducible monitoring of an intracranial stem cell graft (**Figure 7C**, **7D**) [119]. The tetracycline-inducible promoter (Tet-On) was used to control the expression of MagA in mESC, hence controlling the level of MRI contrast. Our study has findings consistent with previous reports: increased iron content with MagA expression and enhanced relaxation rates in MagA-expressing tissue [119]. In one recent study, a MagA transgenic mouse was generated and showed iron accumulation and deposition of nanoparticles in various tissues by MRI [122]. This study also showed no apparent pathological symptoms in any organs and even showed attenuated oxidative damage induced by iron overload [122].

Chemical exchange saturation transfer (CEST): Recently, chemical exchange saturation transfer (CEST), or CEST-MRI, has become an attractive imaging modality with the development of tailored synthetic peptides. Exogenous or endogenous compounds with different resonate frequency from the surrounding water molecules are selectively saturated using radiofrequency (RF) pulses. The saturated signal is subsequently transferred from the compound to surrounding water. The transfer of this saturation is detected through the water signal [123]. Saturation transfer was first measured by Forsen & Hoffman in 1963, by measuring proton transfer rates between salicylaldehyde and water [124]. In 2000, Ward and coworkers reported that many diamagnetic molecules and water protons can be used to enhance the sensitivity to detect low concentration solutes using the process of saturation transfer [125].

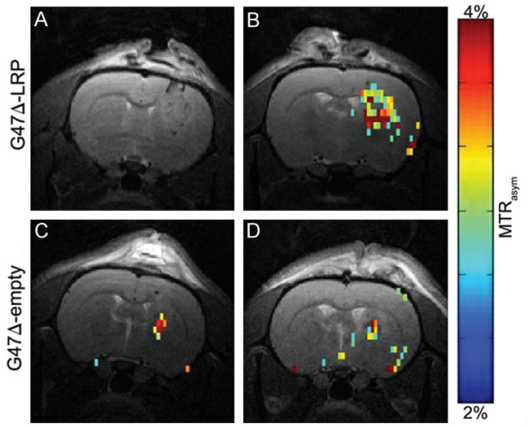

Figure 8. CEST images assess cancer treatment response. Farrar et al., [134] evaluate whether the lysine-rich protein (LRP) MRI reporter gene can be engineered into G47Δ, a herpes simplex-derived oncolytic virus that is currently being tested in clinical trials, and can be in vivo tracked by CEST MRI. Representative MTRasym maps (color scale) acquired with a saturation frequency offset of 3.6 ppm and overlaid onto the associated T2-weighted images at baseline (A and C) and 8 hours after injection of G47Δ-LRP (B) and G47Δ-empty virus (D). A significant increase in MTRasym is observed after virus injection (B) but not in G47Δ-empty virus (D).

CEST-MRI can be explained in a simple two-pool model. Pool water (W) represents the high-concentration (about 110 M) water protons, and Pool solute (S) represents the molecules with the low-concentration (μM-mM range) exchangeable protons, such as hydroxyl, amine, or amide protons. A RF is applied at the resonance frequency of protons in Pool S. Due to difference in saturations, Pool W exchanges saturated protons with protons in Pool S leading to a minute decrease (μM to mM range) in the signal intensity of the protons in Pool W. It should be noted that a single transfer of saturation will not produce significant water signal saturation in Pool W. However, since the Pool W is much larger than the Pool S, each solute proton is replaced by a non-saturated water proton then again saturated. The detectable water signal reduction is generated when the exchange rate of the solute proton is sufficiently fast (more than tens of Hz), and T_1 of water proton is sufficiently long (seconds). This prolonged irradiation causes the accumulation of saturation effect on Pool W. To better understand the basic mechanism of CEST-MRI, we refer the readers to some recent reviews [126-129]. CEST-MRI opens the door for the discovery of endogenous and exogenous molecular contrast agents expanding MRI to multi-frequency detection or "multi-color" imaging [130].

Based on the principle of CEST-MRI, Gilad et al., developed an artificial gene, the lysine-rich protein (LRP), as a CEST-MRI reporter. The LRP provides a high density of amide protons, which can be detected via amide proton CEST-MRI. Through hydrogen bonding, amide proton exchange with bulk water molecules enables detection of LRP rich cells without requiring administration of a cognate probe [131]. LRP was overexpressed by the cytomegalovirus (CMV) promoter and gene-3 promoter (PEG-3 promoter), and an increase of CEST contrast was clearly visible in 9 L tumors model [132]. Using similar CSET contrast strategy, super positively charged mutants of green fluorescent protein (GFP) has also shown a dramatically improved CEST-MRI contrast compared to their wild type counterparts [133].

One of the potential applications of amide proton CEST imaging with the LRP reporter gene is to monitor the migration of the cancer cells as well as tracking stem cells. Oncolytic virus (OV) therapy has been developed in which a replicating virus is injected and selectively enters cancer cells. Therefore, replicated virus either kills the cells or induce an immune reaction capable of killing non-infected cells [134]. Farrar et al. demonstrated that engineered herpes simplex-derived oncolytic virus (G47Δ) carrying LRP reporter gene can be used for CEST imaging without affecting virus efficiency [135]. The process of G47Δ infecting the cell or replicating in tissue could be detected both *in vitro* and *in vivo* by using LRP reporter gene and CEST-MRI (**Figure 8**) [135]. The main strategy is to maximize the saturate-able protons in the Pool S. Therefore, amide group has been used in CEST-MRI. Amide proton transfer-weighted (APTw) image, a CEST-MRI method, has been utilized to show astrogliosis *in vivo* [136].

Despite the attractive features of CEST MRI and its potential to be employed for translational regenerative therapies without the need for exogenous contrast agents [18], it needs further development and investigations to address its limitations in complex post-processing methods and relative low signal-to-noise ratio.

Multimodal imaging approaches

Current developments have focused on molecular probes that allow multimodal imaging, which makes use of two or more imaging techniques (e.g. MRI and PET). The idea of developing multimodal imaging probes is to combine the strengths of the individual imaging modalities, for example the metabolic information or sensitivity from PET with anatomic details of MRI, to overcome the limitations associated with single imaging modalities. Using genetic engineering approaches, fusion proteins are developed as multimodal molecular imaging reporters. Several studies have investigated double or even triple multimodal imaging with fusion protein reporters. The early study reported the development of optical and PET-like hrl-mrfp-ttk [137] or HSV1-TF/GFP/Fluc [138] and showed promising result in monitoring tumor cells *in vivo.* A innovative approach was investigated by Lewis et al. using DMT1. A radioactive isotope of manganese, ^{52}Mn, was produced to track DMT1 over-expressing human neural progenitor cells [139]. However, PET was failed to produce image *in vivo* possibly due to poor biodistribution of ^{52}Mn in the brain while promising result was observed *ex vivo* via autoradiography [139]. Similarly, a tricistronic human norepinephrine transporter (hNET) combined with red-shifted firefly luciferase (Fluc) and a small marker gene RQR8 was used as a BLI/SPECT reporter [140]. The grafted cells were readily visible after administrating ^{123}I-meta-iodobenzyl guanidine (MIBG) [140].

Triple modality molecular imaging capability was demonstrated by Qin et al. [23] using tyrosinase derived genetic reporter. In this system, human breast cancer cells (MCF-7) was transfected with human tyrosinase (TYR), the key enzyme in melanin production. Overproduction of melanin could serve as an excellent imaging probe for photoacoustic imaging (PAI), MRI and PET. Melanin has a broad optical absorption spectrum with significant absorption at near-infrared (NIR) wavelengths, which allows for good tissue penetration. Therefore, it has been demonstrated as an excellent endogenous contrast agent for PAI [141]. Also, melanin has a high affinity for metal ions including Fe^3 [142] thus serve as a promise MRI contrast agent. Finally, a special probe targeting melanin, N-(2-(diethylamino)ethyl)-^{18}F-5-fluoropicolinamide, could be employed for PET imaging. Therefore, this probe can be effectively used to detect TYR reporter gene expression through melanin production [23]. This study provides an excellent example of rational design and use of fusion protein methods to make a genetic engineering reporter for imaging molecular and genetic events in vivo.

Perspectives

With multiple imaging modalities now available for molecular imaging and the unmet need in cell tracking for the development of cell-based therapy, development of molecular imaging reporters for cell tracking remains to be of great interest but with tremendous challenges. Compared to direct labeling methods, indirect endogenous labeling methods have advantages that are critical for stem cell monitoring, including the ability to longitudinally monitor the grafted cells and specificity for rapidly dividing cells. Considering recent stem cell therapy evaluations failed due to poor cell survival, immunological rejections, tumor development, and poor functional integration [143], a reliable genetically engineered MRI reporter will be an important tool, especially when using large animal models in preclinical research. The application of a genetic MRI reporter includes tracking cell migration, proliferation/viability imaging, neurogenesis imaging, myocardial stem cell imaging, cancer stem cell imaging, immune cell imaging, and monitoring of gene expression and differentiation [17, 144, 145]. The monitoring of grafted cells is important regarding evaluating therapeutic efficacy. Due to the limitations associated with current direct and exogenous monitoring methods, a genetic reporter will likely become a key to usher in the successful translation of regenerative medicine.

Other than the previously mentioned concerns (e.g. increasing cytotoxicity and affecting differentiation potential) of expressing a genetic MRI reporter, there are other pitfalls that might be associated with using a genetic MRI reporter. First, since the expression of a reporter gene requires genetic modifications, the integration site of the reporter gene might affect its expression, disrupt normal cell function, be epigenetically silenced, and even promote malignant transformation [17]. One way to overcome this problem is by using targeted gene insertion (knock-in). However, the efficiency of generat-

ing knock-ins is low. Also, inserting non-human gene such as MagA will not be feasible for human clinical applications. However, systems such as ferritin and DMT1 can be used in clinical settings if the safety of the cells expressing those proteins can be ensured. Second, tissue specificity has to be examined especially in stem cells because the expression of the reporter gene later in differentiated cells can be affected by epigenetic silencing. Also, overexpressing a gene, introducing a foreign gene, or increasing iron content in a cell might trigger a host immune response, and immune cells like macrophages might increase iron concentration at the graft site to create a nonspecific signal [17]. As of DMT1, different tissues might have different biodistribution of the contrast agent, which results in low contrast. Therefore, depending on the application and interested organs, the researcher might have to choose the best available method. Third, when an inducible promoter is used, its impact on temporal resolution due to the length of time associated with translating the protein and accumulating enough contrast agents, the turnover rate of the reporter and its clearance have to be investigated [17]. Since the intrinsic limitation of endogenous labeling method is the low sensitivity, multiple strategies can be explored to overcome this problem. The simplest method will be to use more powerful MR scanners. Studies using ferritin have demonstrated a linear increase in contrast enhancement with the increase in the field strength [146]. However, the high field strength scanners (i.e., higher than 7T) may not be available for imaging larger animals or humans. To increase the contrast signal for MRI at the current clinical field strength (i.e., 3T), multiple genes can be expressed. Previously, researchers expressed multiple ferritin/transferrin genes to increase the contrast [147, 148]. Similar methods can be employed for MagA and DMT1 using different combinations of magnetosome-associated genes and iron homeostasis-associated genes. Also, genes can be engineered, so that the resultants proteins can uptake or retain more of contrast agents. Overcoming these limitations will require more investigation involving multidisciplinary efforts.

Conclusions

With the recent growing interest and demand for *in vivo* monitoring of cell grafts, the field of molecular imaging for cell tracking is expected to grow further. With a variety of disease model systems and recent preclinical and clinical trials of stem cell replacement therapies, the tracking of therapeutic cells and monitoring of cell grafts are becoming critical for the future development of these new therapies and strategies. The effort to develop efficient and applicable MRI reporter and novel imaging methods, such as CEST reporter peptide, genetic MRI reporter, and multimodal monitoring methods, are expected to increase significantly. While the clinical translation of imaging reporter may take a long road with more obstacles to overcome, the development of such reporters will indeed enable a further understanding of the basic biology of grafted cells regarding proliferation, survival, migration, differentiation, and functional integration. The eventual development of a safe and effective *in vivo* reporter will help us design better experiments for preclinical studies, and hence facilitate the clinical translation of cell replacement therapy.

Acknowledgements

YNPRC is supported by the National Center for Research Resources P51RR165 and is currently supported by the Office of Research and Infrastructure Program (ORIP)/OD P51OD111-32. This study is supported by a grant awarded by the NINDS/NIH (NS064991) to AWSC.

Disclosure of conflict of interest

None.

Address correspondence to: Dr. Anthony WS Chan, Yerkes National Primate Research Center, Room 2212, Neuroscience Research Building, 954 Gatewood Rd. N.E., Atlanta, GA 30329, USA. E-mail: awchan@emory.edu; Dr. Hui Mao, Department of Radiology and Imaging Sciences, Emory University School of Medicine, 1364 Clifton Road, N.E., Atlanta, GA 30322, USA. E-mail: hmao@emory.edu

References

[1] Thomson JA, Itskovitz-Eldor J, Shapiro SS, Waknitz MA, Swiergiel JJ, Marshall VS and Jones JM. Embryonic stem cell lines derived from human blastocysts. Science 1998; 282: 1145-1147.

[2] Brustle O, Jones KN, Learish RD, Karram K, Choudhary K, Wiestler OD, Duncan ID and McKay RD. Embryonic stem cell-derived glial precursors: a source of myelinating transplants. Science 1999; 285: 754-756.

[3] Reubinoff BE, Pera MF, Fong CY, Trounson A and Bongso A. Embryonic stem cell lines from human blastocysts: somatic differentiation in vitro. Nat Biotechnol 2000; 18: 399-404.
[4] Schuldiner M, Yanuka O, Itskovitz-Eldor J, Melton DA and Benvenisty N. Effects of eight growth factors on the differentiation of cells derived from human embryonic stem cells. Proc Natl Acad Sci U S A 2000; 97: 11307-11312.
[5] Selman K and Kafatos FC. Transdifferentiation in the labial gland of silk moths: is DNA required for cellular metamorphosis? Cell Differ 1974; 3: 81-94.
[6] Davis RL, Weintraub H and Lassar AB. Expression of a single transfected cDNA converts fibroblasts to myoblasts. Cell 1987; 51: 987-1000.
[7] Takahashi K and Yamanaka S. Induction of pluripotent stem cells from mouse embryonic and adult fibroblast cultures by defined factors. Cell 2006; 126: 663-676.
[8] Chung YG, Eum JH, Lee JE, Shim SH, Sepilian V, Hong SW, Lee Y, Treff NR, Choi YH, Kimbrel EA, Dittman RE, Lanza R and Lee DR. Human Somatic Cell Nuclear Transfer Using Adult Cells. Cell Stem Cell 2014; 14: 777-80.
[9] Bachoud-Levi AC, Remy P, Nguyen JP, Brugieres P, Lefaucheur JP, Bourdet C, Baudic S, Gaura V, Maison P, Haddad B, Boisse MF, Grandmougin T, Jeny R, Bartolomeo P, Dalla Barba G, Degos JD, Lisovoski F, Ergis AM, Pailhous E, Cesaro P, Hantraye P and Peschanski M. Motor and cognitive improvements in patients with Huntington's disease after neural transplantation. Lancet 2000; 356: 1975-1979.
[10] Arenas E. Stem cells in the treatment of Parkinson's disease. Brain Res Bull 2002; 57: 795-808.
[11] Park S, Kim EY, Ghil GS, Joo WS, Wang KC, Kim YS, Lee YJ and Lim J. Genetically modified human embryonic stem cells relieve symptomatic motor behavior in a rat model of Parkinson's disease. Neurosci Lett 2003; 353: 91-94.
[12] Lee RH, Seo MJ, Reger RL, Spees JL, Pulin AA, Olson SD and Prockop DJ. Multipotent stromal cells from human marrow home to and promote repair of pancreatic islets and renal glomeruli in diabetic NOD/scid mice. Proc Natl Acad Sci U S A 2006; 103: 17438-17443.
[13] Wernig M, Zhao JP, Pruszak J, Hedlund E, Fu D, Soldner F, Broccoli V, Constantine-Paton M, Isacson O and Jaenisch R. Neurons derived from reprogrammed fibroblasts functionally integrate into the fetal brain and improve symptoms of rats with Parkinson's disease. Proc Natl Acad Sci U S A 2008; 105: 5856-5861.
[14] Schwarz SC and Schwarz J. Translation of stem cell therapy for neurological diseases. Transl Res 2010; 156: 155-160.
[15] Chen Y, Carter RL, Cho IK and Chan AW. Cell-based therapies for Huntington's disease. Drug Discov Today 2014; 19: 980-984.
[16] Carter RL and Chan AW. Pluripotent stem cells models for Huntington's disease: prospects and challenges. J Genet Genomics 2012; 39: 253-259.
[17] Vande Velde G, Himmelreich U and Neeman M. Reporter gene approaches for mapping cell fate decisions by MRI: promises and pitfalls. Contrast Media Mol Imaging 2013; 8: 424-431.
[18] Vandsburger MH, Radoul M, Cohen B and Neeman M. MRI reporter genes: applications for imaging of cell survival, proliferation, migration and differentiation. NMR Biomed 2013; 26: 872-884.
[19] Kircher MF, Gambhir SS and Grimm J. Noninvasive cell-tracking methods. Nat Rev Clin Oncol 2011; 8: 677-688.
[20] Segal AW, Arnot RN, Thakur ML and Lavender JP. Indium-111-labelled leucocytes for localisation of abscesses. Lancet 1976; 2: 1056-1058.
[21] Casadaban MJ, Chou J and Cohen SN. In vitro gene fusions that join an enzymatically active beta-galactosidase segment to amino-terminal fragments of exogenous proteins: Escherichia coli plasmid vectors for the detection and cloning of translational initiation signals. J Bacteriol 1980; 143: 971-980.
[22] Chalfie M, Tu Y, Euskirchen G, Ward WW and Prasher DC. Green fluorescent protein as a marker for gene expression. Science 1994; 263: 802-805.
[23] Qin C, Cheng K, Chen K, Hu X, Liu Y, Lan X, Zhang Y, Liu H, Xu Y, Bu L, Su X, Zhu X, Meng S and Cheng Z. Tyrosinase as a multifunctional reporter gene for Photoacoustic/MRI/PET triple modality molecular imaging. Sci Rep 2013; 3: 1490.
[24] Terrovitis J, Kwok KF, Lautamaki R, Engles JM, Barth AS, Kizana E, Miake J, Leppo MK, Fox J, Seidel J, Pomper M, Wahl RL, Tsui B, Bengel F, Marban E and Abraham MR. Ectopic expression of the sodium-iodide symporter enables imaging of transplanted cardiac stem cells in vivo by single-photon emission computed tomography or positron emission tomography. J Am Coll Cardiol 2008; 52: 1652-1660.
[25] Auricchio A, Acton PD, Hildinger M, Louboutin JP, Plossl K, O'Connor E, Kung HF and Wilson JM. In vivo quantitative noninvasive imaging of gene transfer by single-photon emission computerized tomography. Hum Gene Ther 2003; 14: 255-261.

[26] Cui W, Tavri S, Benchimol MJ, Itani M, Olson ES, Zhang H, Decyk M, Ramirez RG, Barback CV, Kono Y and Mattrey RF. Neural progenitor cells labeling with microbubble contrast agent for ultrasound imaging in vivo. Biomaterials 2013; 34: 4926-4935.
[27] Klibanov AL, Rasche PT, Hughes MS, Wojdyla JK, Galen KP, Wible JH Jr and Brandenburger GH. Detection of individual microbubbles of ultrasound contrast agents: imaging of free-floating and targeted bubbles. Invest Radiol 2004; 39: 187-195.
[28] Welsh DK and Kay SA. Bioluminescence imaging in living organisms. Curr Opin Biotechnol 2005; 16: 73-78.
[29] Bernau K, Lewis CM, Petelinsek AM, Benink HA, Zimprich CA, Meyerand ME, Suzuki M and Svendsen CN. In vivo tracking of human neural progenitor cells in the rat brain using bioluminescence imaging. J Neurosci Methods 2014; 228: 67-78.
[30] Sevick-Muraca EM, Houston JP and Gurfinkel M. Fluorescence-enhanced, near infrared diagnostic imaging with contrast agents. Curr Opin Chem Biol 2002; 6: 642-650.
[31] Frangioni JV. In vivo near-infrared fluorescence imaging. Curr Opin Chem Biol 2003; 7: 626-634.
[32] Ntziachristos V, Bremer C and Weissleder R. Fluorescence imaging with near-infrared light: new technological advances that enable in vivo molecular imaging. Eur Radiol 2003; 13: 195-208.
[33] Koretsky A, Lin Y, Schorle H, Jaenisch R. Genetic control of MRI contrast by expression of the transferrin receptor. Proc ISMRM 1996.
[34] Cohen B, Dafni H, Meir G, Harmelin A and Neeman M. Ferritin as an endogenous MRI reporter for noninvasive imaging of gene expression in C6 glioma tumors. Neoplasia 2005; 7: 109-117.
[35] Liu J, Cheng EC, Long RC, Yang SH, Wang L, Cheng PH, Yang J, Wu D, Mao H and Chan AW. Noninvasive monitoring of embryonic stem cells in vivo with MRI transgene reporter. Tissue Eng Part C Methods 2009; 15: 739-747.
[36] Gilad AA, Ziv K, McMahon MT, van Zijl PC, Neeman M and Bulte JW. MRI reporter genes. J Nucl Med 2008; 49: 1905-1908.
[37] Zurkiya O, Chan AW and Hu X. MagA is sufficient for producing magnetic nanoparticles in mammalian cells, making it an MRI reporter. Magn Reson Med 2008; 59: 1225-1231.
[38] Rohani R, Figueredo R, Bureau Y, Koropatnick J, Foster P, Thompson RT, Prato FS and Goldhawk DE. Imaging Tumor Growth Non-invasively Using Expression of MagA or Modified Ferritin Subunits to Augment Intracellular Contrast for Repetitive MRI. Mol Imaging Biol 2014; 16: 63-73.
[39] Bar-Shir A, Liu G, Chan KW, Oskolkov N, Song X, Yadav NN, Walczak P, McMahon MT, van Zijl PC, Bulte JW and Gilad AA. Human protamine-1 as an MRI reporter gene based on chemical exchange. ACS Chem Biol 2014; 9: 134-138.
[40] Frangioni JV and Hajjar RJ. In vivo tracking of stem cells for clinical trials in cardiovascular disease. Circulation 2004; 110: 3378-3383.
[41] Au KW, Liao SY, Lee YK, Lai WH, Ng KM, Chan YC, Yip MC, Ho CY, Wu EX, Li RA, Siu CW and Tse HF. Effects of iron oxide nanoparticles on cardiac differentiation of embryonic stem cells. Biochem Biophys Res Commun 2009; 379: 898-903.
[42] Wang X, Wei F, Liu A, Wang L, Wang JC, Ren L, Liu W, Tu Q, Li L and Wang J. Cancer stem cell labeling using poly(L-lysine)-modified iron oxide nanoparticles. Biomaterials 2012; 33: 3719-3732.
[43] Blaber SP, Hill CJ, Webster RA, Say JM, Brown LJ, Wang SC, Vesey G and Herbert BR. Effect of labeling with iron oxide particles or nanodiamonds on the functionality of adipose-derived mesenchymal stem cells. PLoS One 2013; 8: e52997.
[44] Rosenberg JT, Sellgren KL, Sachi-Kocher A, Calixto Bejarano F, Baird MA, Davidson MW, Ma T and Grant SC. Magnetic resonance contrast and biological effects of intracellular superparamagnetic iron oxides on human mesenchymal stem cells with long-term culture and hypoxic exposure. Cytotherapy 2013; 15: 307-322.
[45] Chen YC, Hsiao JK, Liu HM, Lai IY, Yao M, Hsu SC, Ko BS, Chen YC, Yang CS and Huang DM. The inhibitory effect of superparamagnetic iron oxide nanoparticle (Ferucarbotran) on osteogenic differentiation and its signaling mechanism in human mesenchymal stem cells. Toxicol Appl Pharmacol 2010; 245: 272-279.
[46] Julke H, Veit C, Ribitsch I, Brehm W, Ludewig E and Delling U. Comparative labelling of equine and ovine multipotent stromal cells with superparamagnetic iron oxide particles for magnetic resonance imaging in vitro. Cell Transplant 2013.
[47] Chung TH, Hsiao JK, Hsu SC, Yao M, Chen YC, Wang SW, Kuo MY, Yang CS and Huang DM. Iron oxide nanoparticle-induced epidermal growth factor receptor expression in human stem cells for tumor therapy. ACS Nano 2011; 5: 9807-9816.
[48] Choi JI, Cho HT, Jee MK and Kang SK. Core-shell nanoparticle controlled hATSCs neurogenesis for neuropathic pain therapy. Biomaterials 2013; 34: 4956-4970.

[49] Shapiro EM, Medford-Davis LN, Fahmy TM, Dunbar CE and Koretsky AP. Antibody-mediated cell labeling of peripheral T cells with micron-sized iron oxide particles (MPIOs) allows single cell detection by MRI. Contrast Media Mol Imaging 2007; 2: 147-153.
[50] Heyn C, Ronald JA, Mackenzie LT, MacDonald IC, Chambers AF, Rutt BK and Foster PJ. In vivo magnetic resonance imaging of single cells in mouse brain with optical validation. Magn Reson Med 2006; 55: 23-29.
[51] Jin Y, Kong H, Stodilka RZ, Wells RG, Zabel P, Merrifield PA, Sykes J and Prato FS. Determining the minimum number of detectable cardiac-transplanted ^{111}In-tropolone-labelled bone-marrow-derived mesenchymal stem cells by SPECT. Phys Med Biol 2005; 50: 4445-4455.
[52] Blackwood KJ, Sabondjian E, Goldhawk DE, Kovacs MS, Wisenberg G, Merrifield P, Prato FS, DeMoor JM and Stodilka RZ. Towards Image-Guided Stem Cell Therapy. Progress in stem cell applications. New York: Nova Science 2008; 153-180.
[53] Zhou R, Thomas DH, Qiao H, Bal HS, Choi SR, Alavi A, Ferrari VA, Kung HF and Acton PD. In vivo detection of stem cells grafted in infarcted rat myocardium. J Nucl Med 2005; 46: 816-822.
[54] Huang M, Batra RK, Kogai T, Lin YQ, Hershman JM, Lichtenstein A, Sharma S, Zhu LX, Brent GA and Dubinett SM. Ectopic expression of the thyroperoxidase gene augments radioiodide uptake and retention mediated by the sodium iodide symporter in non-small cell lung cancer. Cancer Gene Ther 2001; 8: 612-618.
[55] Moroz MA, Serganova I, Zanzonico P, Ageyeva L, Beresten T, Dyomina E, Burnazi E, Finn RD, Doubrovin M and Blasberg RG. Imaging hNET reporter gene expression with ^{124}I-MIBG. J Nucl Med 2007; 48: 827-836.
[56] Kim YH, Lee DS, Kang JH, Lee YJ, Chung JK, Roh JK, Kim SU and Lee MC. Reversing the silencing of reporter sodium/iodide symporter transgene for stem cell tracking. J Nucl Med 2005; 46: 305-311.
[57] Hwang do W, Kang JH, Jeong JM, Chung JK, Lee MC, Kim S and Lee DS. Noninvasive in vivo monitoring of neuronal differentiation using reporter driven by a neuronal promoter. Eur J Nucl Med Mol Imaging 2008; 35: 135-145.
[58] Brenner W, Aicher A, Eckey T, Massoudi S, Zuhayra M, Koehl U, Heeschen C, Kampen WU, Zeiher AM, Dimmeler S and Henze E. ^{111}In-labeled CD34$^+$ hematopoietic progenitor cells in a rat myocardial infarction model. J Nucl Med 2004; 45: 512-518.
[59] Gildehaus FJ, Haasters F, Drosse I, Wagner E, Zach C, Mutschler W, Cumming P, Bartenstein P and Schieker M. Impact of indium-111 oxine labelling on viability of human mesenchymal stem cells in vitro, and 3D cell-tracking using SPECT/CT in vivo. Mol Imaging Biol 2011; 13: 1204-1214.
[60] Zhou R, Acton PD and Ferrari VA. Imaging stem cells implanted in infarcted myocardium. J Am Coll Cardiol 2006; 48: 2094-2106.
[61] Couillard-Despres S, Vreys R, Aigner L and Van der Linden A. In vivo monitoring of adult neurogenesis in health and disease. Front Neurosci 2011; 5: 67.
[62] Belov V, Levine D, Belova E, Mushti C, Bonab A, Fischman A and Papisov M. Pharmacological PET imaging performance with I-124 and Zr-89. J Nucl Med 2014; 55: 590.
[63] Lang C, Lehner S, Todica A, Boening G, Franz WM, Bartenstein P, Hacker M and David R. Positron emission tomography based in-vivo imaging of early phase stem cell retention after intramyocardial delivery in the mouse model. Eur J Nucl Med Mol Imaging 2013; 40: 1730-1738.
[64] Rueger MA, Backes H, Walberer M, Neumaier B, Ullrich R, Simard ML, Emig B, Fink GR, Hoehn M, Graf R and Schroeter M. Noninvasive imaging of endogenous neural stem cell mobilization in vivo using positron emission tomography. J Neurosci 2010; 30: 6454-6460.
[65] Bengel FM, Anton M, Richter T, Simoes MV, Haubner R, Henke J, Erhardt W, Reder S, Lehner T, Brandau W, Boekstegers P, Nekolla SG, Gansbacher B and Schwaiger M. Noninvasive imaging of transgene expression by use of positron emission tomography in a pig model of myocardial gene transfer. Circulation 2003; 108: 2127-2133.
[66] Wolfs E, Holvoet B, Gijsbers R, Casteels C, Roberts SJ, Struys T, Maris M, Ibrahimi A, Debyser Z, Van Laere K, Verfaillie CM and Deroose CM. Optimization of Multimodal Imaging of Mesenchymal Stem Cells Using the Human Sodium Iodide Symporter for PET and Cerenkov Luminescence Imaging. PLoS One 2014; 9: e94833.
[67] Qin C, Lan X, He J, Xia X, Tian Y, Pei Z, Yuan H and Zhang Y. An in vitro and in vivo evaluation of a reporter gene/probe system hERL/^{18}F-FES. PLoS One 2013; 8: e61911.
[68] Shah K and Weissleder R. Molecular optical imaging: applications leading to the development of present day therapeutics. NeuroRx 2005; 2: 215-225.
[69] Contag CH, Spilman SD, Contag PR, Oshiro M, Eames B, Dennery P, Stevenson DK and Benaron DA. Visualizing gene expression in living mammals using a bioluminescent reporter. Photochem Photobiol 1997; 66: 523-531.
[70] Funakoshi S, Miki K, Takaki T, Okubo C, Hatani T, Chonabayashi K, Nishikawa M, Takei I, Oishi

A, Narita M, Hoshijima M, Kimura T, Yamanaka S and Yoshida Y. Enhanced engraftment, proliferation, and therapeutic potential in heart using optimized human iPSC-derived cardiomyocytes. Sci Rep 2016; 6: 19111.
[71] Rice BW, Cable MD and Nelson MB. In vivo imaging of light-emitting probes. J Biomed Opt 2001; 6: 432-440.
[72] Lee KH, Byun SS, Paik JY, Lee SY, Song SH, Choe YS and Kim BT. Cell uptake and tissue distribution of radioiodine labelled D-luciferin: implications for luciferase based gene imaging. Nucl Med Commun 2003; 24: 1003-1009.
[73] Ntziachristos V, Bremer C, Graves EE, Ripoll J and Weissleder R. In vivo tomographic imaging of near-infrared fluorescent probes. Mol Imaging 2002; 1: 82-88.
[74] Kedziorek DA, Solaiyappan M, Walczak P, Ehtiati T, Fu Y, Bulte JW, Shea SM, Brost A, Wacker FK and Kraitchman DL. Using C-arm x-ray imaging to guide local reporter probe delivery for tracking stem cell engraftment. Theranostics 2013; 3: 916-926.
[75] Wu H, Shi H, Zhang H, Wang X, Yang Y, Yu C, Hao C, Du J, Hu H and Yang S. Prostate stem cell antigen antibody-conjugated multiwalled carbon nanotubes for targeted ultrasound imaging and drug delivery. Biomaterials 2014; 35: 5369-5380.
[76] Walczak P, Kedziorek DA, Gilad AA, Barnett BP, Bulte JW. Applicability and limitations of MR tracking of neural stem cells with asymmetric cell division and rapid turnover: The case of the Shiverer dysmyelinated mouse brain. Magn Reson Med 2007; 58: 261-269.
[77] Youn H and Hong KJ. In vivo non invasive molecular imaging for immune cell tracking in small animals. Immune Netw 2012; 12: 223-229.
[78] Kaur D, Rajagopalan S, Chinta S, Kumar J, Di Monte D, Cherny RA and Andersen JK. Chronic ferritin expression within murine dopaminergic midbrain neurons results in a progressive age-related neurodegeneration. Brain Res 2007; 1140: 188-194.
[79] Moats RA, Fraser SE and Meade TJ. A "Smart" Magnetic Resonance Imaging Agent That Reports on Specific Enzymatic Activity. Angew Chem Int Ed Engl 1997; 36: 726-728.
[80] Bulte JW. In vivo MRI cell tracking: clinical studies. AJR Am J Roentgenol 2009; 193: 314-325.
[81] Guenoun J, Koning GA, Doeswijk G, Bosman L, Wielopolski PA, Krestin GP and Bernsen MR. Cationic Gd-DTPA liposomes for highly efficient labeling of mesenchymal stem cells and cell tracking with MRI. Cell Transplant 2012; 21: 191-205.
[82] Hedlund A, Ahren M, Gustafsson H, Abrikossova N, Warntjes M, Jonsson JI, Uvdal K and Engstrom M. Gd(2)O(3) nanoparticles in hematopoietic cells for MRI contrast enhancement. Int J Nanomedicine 2011; 6: 3233-3240.
[83] Agudelo CA, Tachibana Y, Hurtado AF, Ose T, Iida H and Yamaoka T. The use of magnetic resonance cell tracking to monitor endothelial progenitor cells in a rat hindlimb ischemic model. Biomaterials 2012; 33: 2439-2448.
[84] Thomsen HS. Nephrogenic systemic fibrosis: A serious late adverse reaction to gadodiamide. Eur Radiol 2006; 16: 2619-2621.
[85] Kim T, Momin E, Choi J, Yuan K, Zaidi H, Kim J, Park M, Lee N, McMahon MT, Quinones-Hinojosa A, Bulte JW, Hyeon T and Gilad AA. Mesoporous silica-coated hollow manganese oxide nanoparticles as positive T1 contrast agents for labeling and MRI tracking of adipose-derived mesenchymal stem cells. J Am Chem Soc 2011; 133: 2955-2961.
[86] Bengtsson NE, Brown G, Scott EW and Walter GA. lacZ as a genetic reporter for real-time MRI. Magnet Reson Med 2010; 63: 745-753.
[87] Norman AB, Thomas SR, Pratt RG, Lu SY and Norgren RB. Magnetic resonance imaging of neural transplants in rat brain using a superparamagnetic contrast agent. Brain Res 1992; 594: 279-283.
[88] Chung J, Kee K, Barral JK, Dash R, Kosuge H, Wang X, Weissman I, Robbins RC, Nishimura D, Quertermous T, Reijo-Pera RA and Yang PC. In vivo molecular MRI of cell survival and teratoma formation following embryonic stem cell transplantation into the injured murine myocardium. Magnet Reson Med 2011; 66: 1374-1381.
[89] Tannous BA, Grimm J, Perry KF, Chen JW, Weissleder R and Breakefield XO. Metabolic biotinylation of cell surface receptors for in vivo imaging. Nat Methods 2006; 3: 391-396.
[90] Chuang KH, Wang HE, Cheng TC, Tzou SC, Tseng WL, Hung WC, Tai MH, Chang TK, Roffler SR and Cheng TL. Development of a universal anti-polyethylene glycol reporter gene for non-invasive imaging of PEGylated probes. J Nucl Med 2010; 51: 933-941.
[91] Karussis D, Karageorgiou C, Vaknin-Dembinsky A, Gowda-Kurkalli B, Gomori JM, Kassis I, Bulte JW, Petrou P, Ben-Hur T, Abramsky O and Slavin S. Safety and immunological effects of mesenchymal stem cell transplantation in patients with multiple sclerosis and amyotrophic lateral sclerosis. Arch Neurol 2010; 67: 1187-1194.
[92] Gutova M, Frank JA, D'Apuzzo M, Khankaldyyan V, Gilchrist MM, Annala AJ, Metz MZ, Abramyants Y, Herrmann KA, Ghoda LY, Najbauer J, Brown CE, Blanchard MS, Lesniak MS, Kim SU,

Barish ME, Aboody KS and Moats RA. Magnetic resonance imaging tracking of ferumoxytol-labeled human neural stem cells: studies leading to clinical use. Stem Cells Transl Med 2013; 2: 766-775.
[93] Westmeyer GG, Durocher Y and Jasanoff A. A secreted enzyme reporter system for MRI. Angew Chem Int Ed Engl 2010; 49: 3909-3911.
[94] Schmidt R, Nippe N, Strobel K, Masthoff M, Reifschneider O, Castelli DD, Holtke C, Aime S, Karst U, Sunderkotter C, Bremer C and Faber C. Highly shifted proton MR imaging: cell tracking by using direct detection of paramagnetic compounds. Radiology 2014; 272: 785-795.
[95] Weissleder R, Moore A, Mahmood U, Bhorade R, Benveniste H, Chiocca EA and Basilion JP. In vivo magnetic resonance imaging of transgene expression. Nat Med 2000; 6: 351-355.
[96] Frey PA and Reed GH. The ubiquity of iron. ACS Chem Biol 2012; 7: 1477-1481.
[97] Campan M, Lionetti V, Aquaro GD, Forini F, Matteucci M, Vannucci L, Chiuppesi F, Di Cristofano C, Faggioni M, Maioli M, Barile L, Messina E, Lombardi M, Pucci A, Pistello M and Recchia FA. Ferritin as a reporter gene for in vivo tracking of stem cells by 1.5-T cardiac MRI in a rat model of myocardial infarction. Am J Physiol Heart Circ Physiol 2011; 300: H2238-2250.
[98] Naumova AV, Reinecke H, Yarnykh V, Deem J, Yuan C and Murry CE. Ferritin overexpression for noninvasive magnetic resonance imaging-based tracking of stem cells transplanted into the heart. Mol Imaging 2010; 9: 201-210.
[99] Weissleder R, Simonova M, Bogdanova A, Bredow S, Enochs WS and Bogdanov A Jr. MR imaging and scintigraphy of gene expression through melanin induction. Radiology 1997; 204: 425-429.
[100] Bartelle BB, Szulc KU, Suero-Abreu GA, Rodriguez JJ and Turnbull DH. Divalent metal transporter, DMT1: A novel MRI reporter protein. Magn Reson Med 2013; 70: 842-850.
[101] Kolinko I, Lohsse A, Borg S, Raschdorf O, Jogler C, Tu Q, Posfai M, Tompa E, Plitzko JM, Brachmann A, Wanner G, Muller R, Zhang Y and Schuler D. Biosynthesis of magnetic nanostructures in a foreign organism by transfer of bacterial magnetosome gene clusters. Nat Nanotechnol 2014; 9: 193-197.
[102] Goldhawk DE, Rohani R, Sengupta A, Gelman N and Prato FS. Using the magnetosome to model effective gene-based contrast for magnetic resonance imaging. Wiley Interdiscip Rev Nanomed Nanobiotechnol 2012; 4: 378-388.
[103] Richter M, Kube M, Bazylinski DA, Lombardot T, Glockner FO, Reinhardt R and Schuler D. Comparative genome analysis of four magnetotactic bacteria reveals a complex set of group-specific genes implicated in magnetosome biomineralization and function. J Bacteriol 2007; 189: 4899-4910.
[104] Faivre D and Schuler D. Magnetotactic bacteria and magnetosomes. Chem Rev 2008; 108: 4875-4898.
[105] Murat D, Quinlan A, Vali H and Komeili A. Comprehensive genetic dissection of the magnetosome gene island reveals the step-wise assembly of a prokaryotic organelle. Proc Natl Acad Sci U S A 2010; 107: 5593-5598.
[106] Arakaki A, Webb J and Matsunaga T. A novel protein tightly bound to bacterial magnetic particles in Magnetospirillum magneticum strain AMB-1. J Biol Chem 2003; 278: 8745-8750.
[107] Rahn-Lee L and Komeili A. The magnetosome model: insights into the mechanisms of bacterial biomineralization. Front Microbiol 2013; 4: 352.
[108] Zhang XY, Robledo BN, Harris SS and Hu XP. A Bacterial Gene, mms6, as a New Reporter Gene for Magnetic Resonance Imaging of Mammalian Cells. Mol Imaging 2014; 13: 1-12.
[109] Bazylinski DA and Frankel RB. Magnetosome formation in prokaryotes. Nat Rev Microbiol 2004; 2: 217-230.
[110] Nakamura C, Burgess JG, Sode K and Matsunaga T. An iron-regulated gene, magA, encoding an iron transport protein of Magnetospirillum sp. strain AMB-1. J Biol Chem 1995; 270: 28392-28396.
[111] Nakamura C, Kikuchi T, Burgess JG and Matsunaga T. Iron-regulated expression and membrane localization of the magA protein in Magnetospirillum sp. strain AMB-1. J Biochem 1995; 118: 23-27.
[112] Altschul SF, Gish W, Miller W, Myers EW and Lipman DJ. Basic local alignment search tool. J Mol Biol 1990; 215: 403-410.
[113] Bakker EP, Booth IR, Dinnbier U, Epstein W and Gajewska A. Evidence for multiple K+ export systems in Escherichia coli. J Bacteriol 1987; 169: 3743-3749.
[114] Guex N and Peitsch MC. SWISS-MODEL and the Swiss-PdbViewer: an environment for comparative protein modeling. Electrophoresis 1997; 18: 2714-2723.
[115] Kelley LA and Sternberg MJ. Protein structure prediction on the Web: a case study using the Phyre server. Nat Protoc 2009; 4: 363-371.
[116] Goldhawk DE, Lemaire C, McCreary CR, McGirr R, Dhanvantari S, Thompson RT, Figueredo R, Koropatnick J, Foster P and Prato FS. Magnetic resonance imaging of cells overexpressing MagA, an endogenous contrast agent for live cell imaging. Mol Imaging 2009; 8: 129-139.
[117] Sengupta A, Quiaoit K, Thompson RT, Prato FS, Gelman N and Goldhawk DE. Biophysical fea-

tures of MagA expression in mammalian cells: implications for MRI contrast. Front Microbiol 2014; 5: 29.
[118] Bohl D and Heard JM. Tetracycline-Controlled Transactivators and Their Potential Use in Gene Therapy Applications. In: Gossen M, Kaufmann J, Triezenberg S, editors. Transcription Factors. Springer Berlin Heidelberg; 2004. pp. 509-533.
[119] Cho IK, Moran SP, Paudyal R, Piotrowska-Nitsche K, Cheng PH, Zhang X, Mao H, Chan AW. Longitudinal Monitoring of Stem Cell Grafts In Vivo Using Magnetic Resonance Imaging with Inducible MagA as a Genetic Reporter. Theranostics 2014; 4: 972-989.
[120] Feng Y, Liu Q, Zhu J, Xie F and Li L. Efficiency of ferritin as an MRI reporter gene in NPC cells is enhanced by iron supplementation. J Biomed Biotechnol 2012; 2012: 434878.
[121] Cohen B, Ziv K, Plaks V, Israely T, Kalchenko V, Harmelin A, Benjamin LE and Neeman M. MRI detection of transcriptional regulation of gene expression in transgenic mice. Nat Med 2007; 13: 498-503.
[122] Guan X, Jiang X, Yang C, Tian X and Li L. The MRI marker gene MagA attenuates the oxidative damage induced by iron overload in transgenic mice. Nanotoxicology 2015; 1-11.
[123] van Zijl PC and Yadav NN. Chemical exchange saturation transfer (CEST): what is in a name and what isn't? Magn Reson Med 2011; 65: 927-948.
[124] Forsen S and Hoffman RA. Study of moderately rapid chemical exchange reactions by means of nuclear magnetic double resonance. J Chem Phys 1963; 39: 2892-2901.
[125] Ward KM, Aletras AH and Balaban RS. A new class of contrast agents for MRI based on proton chemical exchange dependent saturation transfer (CEST). J Magn Reson 2000; 143: 79-87.
[126] Sherry AD and Woods M. Chemical exchange saturation transfer contrast agents for magnetic resonance imaging. Annu Rev Biomed Eng 2008; 10: 391-411.
[127] Terreno E, Castelli DD and Aime S. Encoding the frequency dependence in MRI contrast media: the emerging class of CEST agents. Contrast Media Mol Imaging 2010; 5: 78-98.
[128] van Zijl PC and Yadav NN. Chemical exchange saturation transfer (CEST): What is in a name and what isn't? Magn Reson Med 2011; 65: 927-948.
[129] Zhou J and van Zijl PC. Chemical exchange saturation transfer imaging and spectroscopy. Progr. NMR Spectr 2006; 48: 109-136.
[130] McMahon MT, Gilad AA, DeLiso MA, Berman SM, Bulte JW, van Zijl PC. New "Multicolor" polypeptide diamagnetic chemical exchange saturation transfer (DIACEST) contrast agents for MRI. Magn Reson Med 2008; 60: 803-812.
[131] Gilad AA, McMahon MT, Walczak P, Winnard PT Jr, Raman V, van Laarhoven HW, Skoglund CM, Bulte JW, van Zijl PC. Artificial reporter gene providing MRI contrast based on proton exchange. Nat Biotechnol 2007; 25: 217-219.
[132] Minn I, Bar-Shir A, Yarlagadda K, Bulte JW, Fisher PB, Wang H, Gilad AA, Pomper MG. Tumor-specific expression and detection of a CEST reporter gene. Magn Reson Med 2015; 74: 544-549.
[133] Bar-Shir A, Liang Y, Chan KW, Gilad AA, Bulte JW. Supercharged green fluorescent proteins as bimodal reporter genes for CEST MRI and optical imaging. Chem Commun (Camb) 2015; 51: 4869-4871.
[134] Russell SJ, Peng KW and Bell JC. Oncolytic virotherapy. Nat Biotechnol 2012; 30: 658-670.
[135] Farrar CT, Buhrman JS, Liu G, Kleijn A, Lamfers ML, McMahon MT, Gilad AA and Fulci G. Establishing the Lysine-rich Protein CEST Reporter Gene as a CEST MR Imaging Detector for Oncolytic Virotherapy. Radiology 2015; 275: 746-754.
[136] Wang S, Tryggestad E, Zhou T, Armour M, Wen Z, Fu DX, Ford E, van Zijl PC and Zhou J. Assessment of MRI parameters as imaging biomarkers for radiation necrosis in the rat brain. Int J Radiat Oncol Biol Phys 2012; 83: e431-436.
[137] Ray P, De A, Min JJ, Tsien RY and Gambhir SS. Imaging tri-fusion multimodality reporter gene expression in living subjects. Cancer Res 2004; 64: 1323-1330.
[138] Ponomarev V, Doubrovin M, Serganova I, Vider J, Shavrin A, Beresten T, Ivanova A, Ageyeva L, Tourkova V, Balatoni J, Bornmann W, Blasberg R and Gelovani Tjuvajev J. A novel triple-modality reporter gene for whole-body fluorescent, bioluminescent, and nuclear noninvasive imaging. Eur J Nucl Med Mol Imaging 2004; 31: 740-751.
[139] Lewis CM, Graves SA, Hernandez R, Valdovinos HF, Barnhart TE, Cai W, Meyerand ME, Nickles RJ and Suzuki M. ^{52}Mn production for PET/MRI tracking of human stem cells expressing divalent metal transporter 1 (DMT1). Theranostics 2015; 5: 227-239.
[140] Badar A, Kiru L, Kalber TL, Jathoul A, Straathof K, Arstad E, Lythgoe MF and Pule M. Fluorescence-guided development of a tricistronic vector encoding bimodal optical and nuclear genetic reporters for in vivo cellular imaging. EJNMMI Res 2015; 5: 18.
[141] Zhang HF, Maslov K, Stoica G and Wang LV. Functional photoacoustic microscopy for high-resolution and noninvasive in vivo imaging. Nat Biotechnol 2006; 24: 848-851.

[142] Hong L and Simon JD. Current understanding of the binding sites, capacity, affinity, and biological significance of metals in melanin. J Phys Chem B 2007; 111: 7938-7947.
[143] Emborg ME, Liu Y, Xi J, Zhang X, Yin Y, Lu J, Joers V, Swanson C, Holden JE and Zhang SC. Induced pluripotent stem cell-derived neural cells survive and mature in the nonhuman primate brain. Cell Rep 2013; 3: 646-650.
[144] Ahrens ET and Bulte JW. Tracking immune cells in vivo using magnetic resonance imaging. Nat Rev Immunol 2013; 13: 755-763.
[145] Youn H and Chung JK. Reporter gene imaging. AJR Am J Roentgenol 2013; 201: W206-214.
[146] Vymazal J, Brooks RA, Zak O, McRill C, Shen C and Di Chiro G. T1 and T2 of ferritin at different field strengths: effect on MRI. Magn Reson Med 1992; 27: 368-374.
[147] Deans AE, Wadghiri YZ, Bernas LM, Yu X, Rutt BK and Turnbull DH. Cellular MRI contrast via coexpression of transferrin receptor and ferritin. Magn Reson Med 2006; 56: 51-59.
[148] Pereira SM, Moss D, Williams SR, Murray P and Taylor A. Overexpression of the MRI Reporter Genes Ferritin and Transferrin Receptor Affect Iron Homeostasis and Produce Limited Contrast in Mesenchymal Stem Cells. Int J Mol Sci 2015; 16: 15481-15496.
[149] Louie AY, Huber MM, Ahrens ET, Rothbacher U, Moats R, Jacobs RE, Fraser SE and Meade TJ. In vivo visualization of gene expression using magnetic resonance imaging. Nat Biotechnol 2000; 18: 321-325.
[150] Sterenczak KA, Meier M, Glage S, Meyer M, Willenbrock S, Wefstaedt P, Dorsch M, Bullerdiek J, Murua Escobar H, Hedrich H and Nolte I. Longitudinal MRI contrast enhanced monitoring of early tumour development with manganese chloride (MnCl2) and superparamagnetic iron oxide nanoparticles (SPIOs) in a CT1258 based in vivo model of prostate cancer. BMC Cancer 2012; 12: 284.
[151] Patel D, Kell A, Simard B, Deng J, Xiang B, Lin HY, Gruwel M and Tian G. Cu2+-labeled, SPION loaded porous silica nanoparticles for cell labeling and multifunctional imaging probes. Biomaterials 2010; 31: 2866-2873.
[152] Neri M, Maderna C, Cavazzin C, Deidda-Vigoriti V, Politi LS, Scotti G, Marzola P, Sbarbati A, Vescovi AL and Gritti A. Efficient in vitro labeling of human neural precursor cells with superparamagnetic iron oxide particles: relevance for in vivo cell tracking. Stem Cells 2008; 26: 505-516.
[153] Boni A, Ceratti D, Antonelli A, Sfara C, Magnani M, Manuali E, Salamida S, Gozzi A and Bifone A. USPIO-loaded red blood cells as a biomimetic MR contrast agent: a relaxometric study. Contrast Media Mol Imaging 2014; 9: 229-236.
[154] Kircher MF, Allport JR, Graves EE, Love V, Josephson L, Lichtman AH and Weissleder R. In vivo high resolution three-dimensional imaging of antigen-specific cytotoxic T-lymphocyte trafficking to tumors. Cancer Res 2003; 63: 6838-6846.
[155] Sibov TT, Pavon LF, Miyaki LA, Mamani JB, Nucci LP, Alvarim LT, Silveira PH, Marti LC and Gamarra L. Umbilical cord mesenchymal stem cells labeled with multimodal iron oxide nanoparticles with fluorescent and magnetic properties: application for in vivo cell tracking. Int J Nanomedicine 2014; 9: 337-350.
[156] Hitchens TK, Liu L, Foley LM, Simplaceanu V, Ahrens ET and Ho C. Combining perfluorocarbon and superparamagnetic iron-oxide cell labeling for improved and expanded applications of cellular MRI. Magn Reson Med 2015; 73: 367-75.
[157] Ahrens ET and Zhong J. In vivo MRI cell tracking using perfluorocarbon probes and fluorine-19 detection. NMR Biomed 2013; 26: 860-871.
[158] Walling MA, Novak JA and Shepard JR. Quantum dots for live cell and in vivo imaging. Int J Mol Sci 2009; 10: 441-491.
[159] Sutton EJ, Henning TD, Pichler BJ, Bremer C and Daldrup-Link HE. Cell tracking with optical imaging. Eur Radiol 2008; 18: 2021-2032.
[160] Bass LA, Wang M, Welch MJ and Anderson CJ. In vivo transchelation of copper-64 from TETA-octreotide to superoxide dismutase in rat liver. Bioconjug Chem 2000; 11: 527-532.
[161] Moore A, Basilion JP, Chiocca EA and Weissleder R. Measuring transferrin receptor gene expression by NMR imaging. Biochim Biophys Acta 1998; 1402: 239-249.
[162] Severance S, Chakraborty S and Kosman DJ. The Ftr1p iron permease in the yeast plasma membrane: orientation, topology and structure-function relationships. Biochem J 2004; 380: 487-496.
[163] Oh HJ, Hwang do W, Youn H and Lee DS. In vivo bioluminescence reporter gene imaging for the activation of neuronal differentiation induced by the neuronal activator neurogenin 1 (Ngn1) in neuronal precursor cells. Eur J Nucl Med Mol Imaging 2013; 40: 1607-1617.
[164] MacLaren DC, Gambhir SS, Satyamurthy N, Barrio JR, Sharfstein S, Toyokuni T, Wu L, Berk AJ, Cherry SR, Phelps ME and Herschman HR. Repetitive, non-invasive imaging of the dopamine D2 receptor as a reporter gene in living animals. Gene Ther 1999; 6: 785-791.
[165] Wang L, Tang K, Zhang Q, Li H, Wen Z, Zhang H and Zhang H. Somatostatin receptor-based molecular imaging and therapy for neuroendocrine tumors. Biomed Res Int 2013; 2013: 102819.

[166] Uebe R, Junge K, Henn V, Poxleitner G, Katzmann E, Plitzko JM, Zarivach R, Kasama T, Wanner G, Posfai M, Bottger L, Matzanke B and Schuler D. The cation diffusion facilitator proteins MamB and MamM of Magnetospirillum gryphiswaldense have distinct and complex functions, and are involved in magnetite biomineralization and magnetosome membrane assembly. Mol Microbiol 2011; 82: 818-835.

[167] Raschdorf O, Muller FD, Posfai M, Plitzko JM and Schuler D. The magnetosome proteins MamX, MamZ and MamH are involved in redox control of magnetite biomineralization in Magnetospirillum gryphiswaldense. Mol Microbiol 2013; 89: 872-886.

[168] Li Y, Bali S, Borg S, Katzmann E, Ferguson SJ and Schuler D. Cytochrome cd1 nitrite reductase NirS is involved in anaerobic magnetite biomineralization in Magnetospirillum gryphiswaldense and requires NirN for proper d1 heme assembly. J Bacteriol 2013; 195: 4297-4309.

[169] Li Y, Katzmann E, Borg S and Schuler D. The periplasmic nitrate reductase nap is required for anaerobic growth and involved in redox control of magnetite biomineralization in Magnetospirillum gryphiswaldense. J Bacteriol 2012; 194: 4847-4856.

[170] Siponen MI, Adryanczyk G, Ginet N, Arnoux P and Pignol D. Magnetochrome: a c-type cytochrome domain specific to magnetotatic bacteria. Biochem Soc Trans 2012; 40: 1319-1323.

[171] Scheffel A, Gardes A, Grunberg K, Wanner G and Schuler D. The major magnetosome proteins MamGFDC are not essential for magnetite biomineralization in Magnetospirillum gryphiswaldense but regulate the size of magnetosome crystals. J Bacteriol 2008; 190: 377-386.

[172] Komeili A, Li Z, Newman DK and Jensen GJ. Magnetosomes are cell membrane invaginations organized by the actin-like protein MamK. Science 2006; 311: 242-245.